

Synchronization Methods for Wavelet Packet Multicarrier Modulation

M.Sc Thesis

Submitted by:

RAHMAT MULYAWAN

(Student ID: 4124480)

Supervisor:

Dr. Homayoun Nikookar

Mentor:

Madan Kumar Lakshmanan, M.Sc



International Research Center for Telecommunications and Radar

Department of Electrical Engineering, Mathematics and Computer Science

Delft University of Technology

Mekelweg 4, 2628 CD Delft, The Netherlands

August, 2011

Synchronization Methods for Wavelet Packet Multicarrier Modulation

by:

Rahmat Mulyawan

M.Sc Thesis

Presented to the Faculty of the Graduate School of

Technische Universiteit Delft

In Partial Fulfillment of the Requirements

for the Degree of

Master of Science in Telecommunication

Technische Universiteit Delft

August 2011

Abstract

Wavelet Packet based Multi-Carrier Modulation (WPM) offers an alternative to the well-established Orthogonal Frequency Division Multiplexing (OFDM) as an efficient multicarrier modulation technique. It has strong advantage of being generic transmission scheme whose actual characteristics can be widely customized to fulfill several requirements and constraints of advanced communication systems. In the last decades wavelets have been favorably applied in signal and image processing fields but they just recently attracted attention of the telecommunication community. Therefore, some research questions remain to be addressed before novel WPM can be used in practice. One of the major concerns involves the performance of WPM transceivers under various synchronization errors. In this thesis we analyze the interference in WPM transmission caused by the carrier frequency offset and time synchronization errors. Using standard wavelets, the sensitivity of WPM transceivers to these errors is evaluated through simulation studies and their performances are compared and contrasted to OFDM. To alleviate the WPM's vulnerability to time synchronization errors, a method of synchronization is proposed. The proposed time synchronization method in WPM is based on already published feed-forward decision-directed approach which uses correlation method in the wavelet domain (after processed by the analysis filter bank in the receiver side), with lower implementation complexity and improved stability. The proposed method can be considered as "coarse" time synchronization, suitable for estimating large time offset but with less precision. Through computer simulations the performance of the proposed method is proven and further its performance is compared for different parameters of wavelet filters.

Acknowledgement

First, I would like to express my gratitude to my supervisor Dr. H.Nikookar for offering invaluable assistance, expertise and guidance. I greatly benefited from the many informative and enjoyable discussions I have had with him. I would also like to thank my mentor M.K.Lakshmanan, M.Sc. whose friendship, continued assistance, stimulating suggestions and encouragement helped me throughout the course of this work. Both of them have encouraged me to pursue my interests in academic and non-academic, and this has been a primary factor in making my stay at Delft enjoyable.

I thank Erasmus Mundus for granting me the Erasmus Mundus Mobility for Life Scholarship. The scholarship covered the educational expenses for my study at TUD. I also thank Indonesian Ministry of Education for granting me the Excellence Scholarship Program. With this generous support I can finally finish my study in The Netherlands in a good shape. My special thanks are due to Prof. Leo P. Lighart and Dr. Suhartono Tjondronegoro for their help through the application procedure for these scholarships.

Thanks also to all my lab mates at the IRCTR - Mark, Pablo, Stephan, Tom for the many interesting discussions and the relaxed atmosphere in the office. I deeply cherish all the fantastic times I have had interacting with my fellow international students, Anurag, Deepak, Sanju, Bhimo. They have been inspirational and conversations with them have always been enlightening.

Outside of the TUD campus, I have found great comfort and support from many kind people. Especially my roommates at Nicolaas: Mr. Agung, Kiai Asrof, Pras and Pandu for all the best time of Ramadhan in Netherlands. Special thanks to Wahyu who has been a caring friend and has always provided a different perspective on life.

Finally, I dedicate this work to my parents Mazerang and Rahmatiah, my wife Ramlah, and my son Syathir. Without their unwavering and unconditional love, affection, support and sacrifice, I would have never embarked on my Masters study.

Table of Contents

1	Introduction.....	13
1.1	OFDM and WPM	13
1.2	Synchronization in WPM	16
1.3	Objectives and Novelty of the Thesis	17
1.4	Outline of the Thesis.....	17
2	Wavelet Theory	19
2.1	The History of Wavelet	19
2.2	Continuous Wavelet Transform.....	21
2.3	Discrete Wavelet Transform.....	22
2.4	Multiresolution Analysis	24
2.5	Filter Banks.....	27
2.5.1	Analysis Filter Bank	28
2.5.2	Synthesis Filter Bank	31
2.6	Wavelet Packets.....	32
2.6.1	Wavelets Families.....	35
2.6.2	Wavelet Packet based Multicarrier Modulation	39
2.7	Summary of Wavelet Theory.....	42
3	Synchronization Impairments	43
3.1	Time Offset in Multicarrier Modulation.....	44
3.1.1	Time Offset in OFDM	45
3.1.2	Time Offset in WPM	47
3.1.3	Numerical Results for Time Offset.....	48
3.2	Frequency Offset in Multicarrier Modulation	53
3.2.1	Frequency Offset in OFDM.....	54
3.2.2	Frequency Offset in WPM.....	54
3.2.3	Numerical results for Frequency Offset.....	55
3.3	Summary of Synchronization Impairments	61

4	Synchronization in WPM	63
4.1	Time Synchronization in WPM.....	63
4.1.1	Recent Works in Time Synchronization for WPM	63
4.1.2	Proposed Method for Time Synchronization in WPM.....	66
4.1.3	Numerical Results	69
4.2	Frequency Synchronization in WPM	75
4.3	Summary of WPM Synchronization	78
5	Conclusion.....	79
5.1	Key Research Conclusions.....	79
5.2	Recommendations for Further Research	80
	Bibliography.....	82

List of Figures

Figure 1-1: SC vs MC Modulation	14
Figure 1-2 : OFDM spectrum with 8 subcarriers.....	14
Figure 1-3 : WPM spectrum with 8 subcarriers.....	15
Figure 1-4 : OFDM symbol with CP	16
Figure 2-1 : Spaces Spanned by the Scaling Functions	25
Figure 2-2 : Spaces Spanned by the Scaling Functions and Wavelets	26
Figure 2-3 : Frequency response using Daubechies filter with length 8.....	27
Figure 2-4 : Analysis Filter Bank	29
Figure 2-5 : 3-Stage Analysis Filter Banks.....	30
Figure 2-6 : Frequency Bands for 3-Stage Analysis Filter Banks	30
Figure 2-7 : Synthesis Filter Bank	31
Figure 2-8 : 3-Stage Synthesis Filter Banks	32
Figure 2-9 : Frequency Bands for 3-Stage Wavelet Packets Tree	33
Figure 2-10 : 3-Stage Wavelet Packets Analysis Tree.....	34
Figure 2-11 : 3-Stage Wavelet Packets Synthesis Tree	35
Figure 2-12 : Haar Wavelets.....	36
Figure 2-13 : Daubechies Wavelets	37
Figure 2-14 : Biorthogonal Wavelets.....	37
Figure 2-15 : Coiflets Wavelets	38
Figure 2-16 : Symlets Wavelets.....	38
Figure 2-17 : M-band Transmultiplexer structure	40
Figure 3-1 : Timing offset away from CP (to the right)	45
Figure 3-2 : Timing offset towards the CP (to the left)	46
Figure 3-3 : WPM Time Offset Performance with Various Filter Length.....	49
Figure 3-4 : WPM Time Offset Performance with Various Number of Subcarriers	50
Figure 3-5 : WPM Time Offset Performance with Various Number of Symbols	51
Figure 3-6 : WPM Time Offset Performance with Various Time Offsets.....	52
Figure 3-7 : WPM Frequency Offset Performance with Various Filter Length	56
Figure 3-8 : WPM Frequency Offset Performance with Various Number of Subcarriers	57
Figure 3-9 : WPM Frequency Offset Performance with Various Number of Symbols.....	58
Figure 3-10 : WPM Frequency Offset Performance with Various Frequency Offsets.....	59
Figure 4-1 : Architecture of the M&M multicarrier timing offset estimator	65
Figure 4-2 : Fractional time offset estimates of WPM (db6, 16 subcarriers)	66
Figure 4-3 : WPM Symbol Synchronization Block Diagram.....	67

Figure 4-4 : Time Estimation with Time Offset = 2 and SNR: 30, 20, 10, and 5 dB.....	70
Figure 4-5 : Time Estimation with Time Offset = 2 and SNR: 0, -5, -10, and -20 dB.....	71
Figure 4-6 : Percentage of Successful Estimation vs SNR	72
Figure 4-7 : Percentage of Successful Estimation for Different Wavelet Filter Length	73
Figure 4-8 : Average BER for Different Wavelet Filter Length	74
Figure 4-9 : Mean Square Error for Different Wavelet Filter Length	74
Figure 4-10 : Farrow Structure of the Polynomial Interpolator	75
Figure 4-11 : M&M algorithm with correlation per subband basis.....	76
Figure 4-12 : M&M algorithm with correlation utilizes all subcarriers of the subbands	76
Figure 4-12 : S-curve of CFO estimator with perfect decisions and zero phase error	77

List of Tables

Table 2-1 : Wavelet Families Properties.....	39
Table 3-1 : WPM Time Offset Simulation with Various Filter Length.....	49
Table 3-2 : WPM Time Offset Simulation with Various Number of Subcarriers	50
Table 3-3 : WPM Time Offset Simulation with Various Number of Symbols	51
Table 3-4 : WPM Time Offset Simulation with Various Time Offsets.....	52
Table 3-5 : WPM Frequency Offset Simulation with Various Filter Length	56
Table 3-6 : WPM Frequency Offset Simulation with Various Number of Subcarriers.....	57
Table 3-7 : WPM Frequency Offset Simulation with Various Number of Symbols	58
Table 3-8 : WPM Frequency Offset Simulation with Various Frequency Offsets.....	59
Table 4-1 : WPM Time Synchronization Simulation 1	70
Table 4-2 : WPM Time Synchronization Simulation 2	72
Table 4-3 : WPM Frequency Synchronization Simulation.....	77

List of Abbreviations

AWGN	Additive White Gaussian Noise
BER	Bit Error Rate
CFO	Carrier Frequency Offset
CMFB	Cosine Modulated Filter Bank
CP	Cyclic Prefix
CWT	Continous Wavelet Transform
DAB	Digital Audio Broadcasting
DFT	Discrete Fourier Transform
DSL	Digital Subscriber Line
DVB	Digital Video Broadcasting
DWPT	Discrete Wavelet Packet Transform
DWT	Discrete Wavelet Transform
FFT	Fast Fourier Transform
FIR	Finite Impulse Response
ICI	Inter-Carrier Interference
IDFT	Inverse Discrete Fourier Transform
IDWPT	Inverse Discrete Wavelet Packet Transform
IDWT	Inverse Wavelet Packet Transform
ISI	Inter-Symbol Interference
MC	Multi Carrier
M&M	Mueller and Muller (Algorithm)
MLDD	Maximum Likelihood Decision Directed
MRA	Multi-Resolution Analysis
MSE	Mean Square Error
OFDM	Orthogonal Frequency Division Multiplexing
QPSK	Quadrature Phase Shift Keying
SC	Single Carrier
SNR	Signal to Noise Ratio
WPM	Wavelet Packet Modulation

List of Symbols

α	Discrete Scale Index
a_k	Constellation Symbols
$\hat{a}_{i,k}$	k -th Symbol Decision from the i -th Analysis Subband
β	Discrete Translation Index
$\delta\tau_k$	Estimates of Timing Offset on subcarrier k
$\Delta\tau_{MM}$	Estimates of Timing Offset in Mueller & Muller Algorithm
ΔfT	Normalized Frequency Offset
ζ	Discrete Wavelet Packet Transform Coefficients
κ	Continuous Scale
λ, γ	Discrete Wavelet Transform Coefficients
μ_M	Step Size with Mueller & Muller based Frequency Acquisition
ξ	WPM subcarriers
τ	Maximum Likelihood Timing Estimator
φ	Scaling Function
χ	Continuous Translation
ψ	Wavelet Function
f	Frequency
$\ f\ ^2$	Energy of the input signal $f(t)$
g	Wavelet Filter Coefficients (HPF)
g_i	Known Channel Attenuation Factor for the i -th Analysis Subband
G	Wavelet Filter (Analysis)
G	Wavelet Filter (Synthesis)
h	Scaling Filter Coefficients (LPF)
$h_{i,n}$	Cascaded Filter Impulse Response of the i -th Analysis Subband
H	Scaling Filter (Analysis)
H	Scaling Filter (Synthesis)
K	Observation Window Size (Symbols) in MLDD Estimation
l	Level in the Wavelet Packet Tree
M	Number of Subbands in MLDD Estimation
N	Number of Subcarriers
N_{CP}	Length of Cyclic Prefix
N_s	Number of Samples per WPM pulse

p, k	Subcarrier Index
R	Received Signal
R_s	Data Rate
S	Transmitted Signal
t	Time Instance
T	Duration of Symbols (Single Carrier)
T_{MC}	Duration of Symbols (Multi Carrier)
$y_{i,k}$	k -th Received Complex Symbol from the i -th Analysis Subband
y_n	n -th Sampled Complex Output from the Receiver Matched Filter

1 INTRODUCTION

The telecommunication market has progressed rapidly in the last decades, creating a need for new techniques that can accommodate high data rates. Many digital communications services have been deployed with constantly growing data rates like digital radio, digital television, and mobile Internet. In conventional single-carrier (SC) communication systems, the data is transmitted sequentially and therefore the data rate R_s is inversely proportional to the duration of each symbol, this means higher data rates will result in shorter symbol duration. The problem arises in dispersive channels when the duration of transmitted symbols becomes shorter compared to the delay introduced by the channel. As a result, the received symbols are widely spread in time and causing Inter Symbol Interference (ISI). The amount of ISI in a given channel increases for growing data rate R_s limiting the connection speed. Today, WCDMA is one of the fastest single carrier solutions on the market that can operate in dispersive environments at a rate of 3.84 Mchips/s.

1.1 OFDM and WPM

The problem of ISI in SC can be solved by using Multi-Carrier Modulation (MC) technique. MC systems divide the total bandwidth in N narrow channels, which are transmitted in parallel. The original data stream at rate R_s is divided into N streams each having data rate of R_s/N and therefore N times longer symbol duration, i.e. $T_{MC} = NT$. Each data symbol in SC systems occupies the entire available bandwidth while an individual data symbol in MC system only occupies a fraction of the total bandwidth. Therefore, narrow band interference or strong frequency band attenuation can cause SC transmission to completely fail but in MC they only affect subcarriers located at particular frequencies.

One of the most popular MC implementation is Orthogonal Frequency Division Multiplexing (OFDM), due to its spectrally efficient transmission. OFDM has caught a lot of attention since the growth of high data rate applications has caused spectrum to become scarce. Because of its efficient bandwidth utilization, OFDM is now the most commonly used MC modulation technique and is widely adopted across the world.

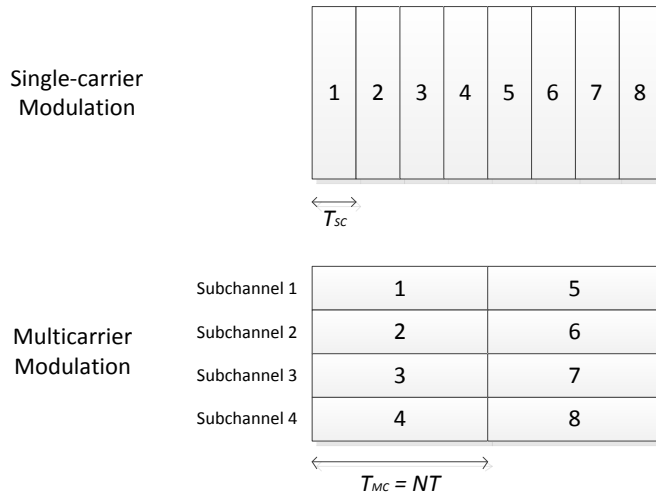


Figure 1-1: SC vs MC Modulation

Among the systems which employ OFDM techniques are European Digital Audio Broadcasting (DAB), Digital Video Broadcasting (DVB), WiFi (IEEE 802.11a/g/j/n), and most recently WiMAX (IEEE 802.16). The high spectral efficiency of OFDM is due to its orthogonal subcarriers which allow their spectrums to overlap. Adjacent subcarriers do not interfere with each other as long as they preserve their orthogonality. Figure 1-2 illustrates this with the spectrum of OFDM for 8 subcarriers.

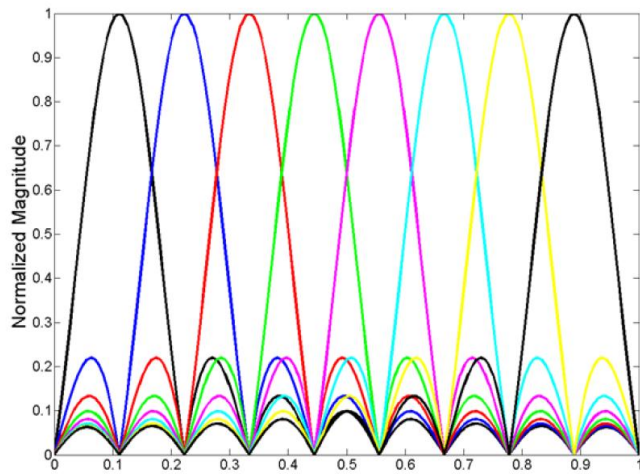


Figure 1-2 : OFDM spectrum with 8 subcarriers

But even with all of its advantages, OFDM doesn't solve the problem of radio spectrum scarcity as popularity of the wireless services keep increasing every day. Currently, most spectrum has been allocated and it is becoming increasingly difficult to find frequency bands that can be made available

either for new services or to expand existing ones. Even while available frequency bands appear to be fully occupied, a FCC study conducted in 2002 revealed that much of the available spectrum lies fallow most of the time (20% or less of the spectrum is used) and that spectrum congestions are more due to the sub-optimal use of spectrum than to the lack of free spectrum [1].

One possible solution to this problem is introduced in the late 90's as an intelligent communication system that estimates the channel and adaptively reconfigures to maximize resource utilization, known as Cognitive Radio [2]. MC modulation is recognized as a good platform for Cognitive Radio as the subcarriers located in the frequency bands occupied by legitimate users can be easily cancelled. OFDM with desirable properties like spectral efficiency and robustness against channel fading and dispersion is one of the possible candidates. However, OFDM employ static subcarriers offering little flexibility and moreover each subcarrier has large side-lobes requiring meticulous filtering and sufficient guard bands.

Recently Wavelet Packet based Multi-Carrier Modulation (WPM) has been propounded as an alternative to the OFDM [3]-[6]. Also similar to OFDM, WPM employs orthogonal subcarriers which spectra is overlapping each other, resulting in high spectral efficiency. But the greatest motivation for pursuing WPM system lies in the flexibility they offer and excellent frequency selectivity. Because WPM can be efficiently implemented by an iterative method the number of subcarriers and their bandwidth can be easily changed. Furthermore the specifications of WPM can be tailored according to the engineering requirement by just altering the filter coefficients. Using frequency selective filters subcarriers with much lower side-lobes than those of OFDM can be obtained allowing better mitigation of interference [7].

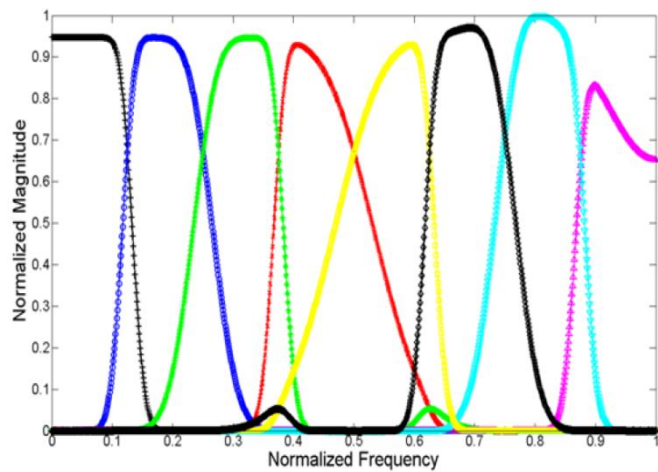


Figure 1-3 : WPM spectrum with 8 subcarriers

However, some key research questions remain to be addressed before WPM can become practically implemented. One of the major concerns involves sensitivity and vulnerability of WPM transceivers to the synchronization errors, since it is known that those types of errors can destroy orthogonality in spectral efficient multicarrier systems and cause interference. Unlike OFDM, wavelets have just recently emerged as a MC modulation technique there is little known about their sensitivity to synchronization errors and local oscillators' imperfections. This has motivated us to investigate the effect of synchronization errors on WPM transmission, as well as the way to mitigate those problems.

1.2 Synchronization in WPM

Due to delay spread of the channel, MC symbols could overlap one another in time, a phenomenon known as Inter-Symbol Interference (ISI), and perfect reconstruction in the receiver may not be possible. To decrease amount of ISI in dispersive channels, OFDM insert guard intervals between its symbols. Usually in OFDM the cyclic prefix (CP) is used as it makes the OFDM signal appear periodic and therefore avoid the discrete time property of the convolution.

The cyclic prefix is a copy of last N_{CP} samples of OFDM symbols which is appended to the front of each symbol. The effect of the dispersive channels can be efficiently mitigated if the length of a cyclic prefix is set longer than the span of the channel. Figure 1-4 illustrates an OFDM symbol with cyclic prefix.

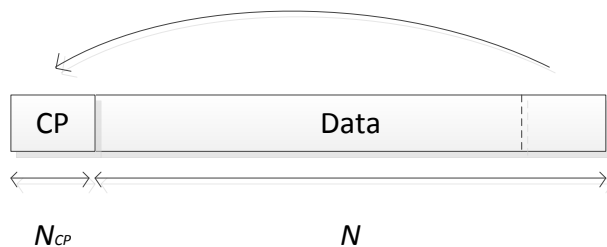


Figure 1-4 : OFDM symbol with CP

The use of CP has been very beneficial in developing synchronization techniques for OFDM. Not only increase the robustness against channel spreading, CP also become the basic foundation in many OFDM synchronization techniques. Unfortunately WPM can't have any of this luxury due to the nature of its overlapping symbols in time domain. But from WPM perspectives, the absence of CP also give certain benefit; because cyclic prefix doesn't contain any useable data it decreases the spectral efficiency in OFDM, while WPM without CP can fully utilize its spectral efficiency.

1.3 Objectives and Novelty of the Thesis

The primary objectives of this thesis work are:

- To study the characteristics of WPM and its possible synchronization techniques.
- To evaluate the performance degradation of WPM transceiver in the presence of carrier frequency offset and symbol time synchronization error.
- To devise suitable algorithms to estimate time and frequency offsets and maintain the transceiver synchronization.
- To evaluate the performance of the proposed synchronization algorithm.

1.4 Outline of the Thesis

This chapter 1 provide a brief introduction to OFDM and WPM synchronization. Theoretical foundation of wavelet transformation is described in chapter 2. The first section of chapter 2 discusses the history of wavelet, continued by the basic idea of continuous and also discrete wavelet transform, in order to work in finite time domain. Using the underlying principle of multi resolution analysis the discrete wavelet transform is practically realized by the filter banks. At this stage the wavelet packed are introduced and their composition and decomposition is discussed using analysis and synthesis filter banks, respectively. After discussing all theoretical elements, the block diagram of WPM is illustrated for the transmitter and receiver. Furthermore, in this chapter we show some standard wavelets that can be used in WPM transceivers and give their specifications.

The synchronization impairments like time offset and frequency offset are discussed in chapter 3. For each of these synchronization errors a model is presented and theoretical analysis is given for both WPM and OFDM. The Bit Error Rate (BER) performance under time offset and frequency offset is investigated by means of simulations studies. The simulations are performed for WPM with different types of parameters and compared to OFDM.

After analyzing the synchronization impairments, the mitigation methods are addressed in chapter 4. Recent works in WPM synchronization are discussed in the beginning of this chapter, followed by the discussion about algorithms in time offset and frequency offset estimation. The performance of WPM with utilization of synchronization algorithm is examined by simulations with various parameters.

Finally, chapter 5 gives a short summary of the work done and concludes the thesis. The recommendations for the further work on WPM can also be found at the end of chapter 5.

2 WAVELET THEORY

The wavelet theory is very much related to Fourier analysis. In fact, it can be viewed as an extension of Fourier analysis because the basic idea of both transformations is the same: representing a function by a set of other functions. In 1800s Joseph Fourier discovered that he could superpose sinusoidal functions to represent other functions. Since then Fourier analysis has been used extensively by scientists and engineers for all kind of problems and applications. However, Fourier analysis does not work equally well for each problem. Fourier analysis is much more useful to solve linear problem and observe stationary signals, while it is rendered almost ineffective when dealing with brief, unpredictable and non-stationary signals. This is where the Wavelet Transform enter the stage.

The wavelets are a relatively new concept that has been introduced in the 1980s although some pioneering work had been done earlier. Since the 1980s wavelets have attracted considerable interest from the theoreticians and engineers where wavelets have promising applications. Because of the large interest, the wavelet theory has been well developed over the past years and several books on this subject have appeared as well as a large volume of research articles.

2.1 The History of Wavelet

In the history, wavelet analysis shows many different origins. Much of the work was performed in the 1930s, and, at the time, the separate efforts did not appear to be parts of a coherent theory.

Pre-1930

Before 1930, the main branch of mathematics leading to wavelets began with Joseph Fourier (1807) with his theories of frequency analysis, now often referred to as Fourier synthesis. He asserted that any 2π -periodic function $f(x)$ is the sum of its Fourier series:

$$a_0 + \sum_{k=1}^{\infty} (a_k \cos kx + b_k \sin kx) \quad (2.1)$$

where $a_0 = \frac{1}{2\pi} \int_0^{2\pi} f(x) dx$, $a_k = \frac{1}{\pi} \int_0^{2\pi} f(x) \cos(kx) dx$, and $b_k = \frac{1}{\pi} \int_0^{2\pi} f(x) \sin(kx) dx$

Fourier's assertion played an essential role in the evolution of the ideas mathematicians had about the functions. He opened up the door to a new functional universe.

After 1807, by exploring the meaning of functions, Fourier series convergence, and orthogonal systems, mathematicians gradually were led from their previous notion of *frequency analysis* to the notion of *scale analysis*. That is, analyzing $f(x)$ by constructing a function, shifting it by some amount, and changing its scale. Then applying that structure in approximating a signal and repeating the procedure. It turns out that this sort of scale analysis is less sensitive to noise because it measures the average fluctuations of the signal at different scales.

The first mention of wavelets appeared in an appendix to the thesis of A. Haar (1909). One property of the Haar wavelet is that it has *compact support*, which means that it vanishes outside of a finite interval. Unfortunately, Haar wavelets are not continuously differentiable which somewhat limits their applications.

The 1930s

In the 1930s, several groups working independently researched the representation of functions using *scale-varying basis functions*. Those are basis functions that varies in scale by chopping up the same function or data space using different scale sizes. For example, imagine we have a signal over the domain from 0 to 1. We can divide the signal with two step functions that range from 0 to $\frac{1}{2}$ and $\frac{1}{2}$ to 1. Then we can divide the original signal again using four step functions from 0 to $\frac{1}{4}$, $\frac{1}{4}$ to $\frac{1}{2}$, $\frac{1}{2}$ to $\frac{3}{4}$, and $\frac{3}{4}$ to 1. And so on. Each set of representations code the original signal with a particular resolution or scale.

By using a scale-varying basis function called the Haar basis function Paul Levy, a 1930s physicist, investigated Brownian motion, a type of random signal. He found the Haar basis function superior to the Fourier basis functions for studying small complicated details in the Brownian motion.

Another 1930s research effort by Littlewood, Paley, and Stein involved computing the energy of a periodic signal f :

$$\text{energy} = \frac{1}{2} \int_0^{2\pi} |f(x)|^2 dx \quad (2.2)$$

The computation produced different results if the energy was concentrated around a few points or distributed over a larger interval. This result disturbed the scientists because it indicated that energy might not be conserved. The researchers discovered a function that can vary in scale *and* can conserve energy when computing the functional energy. Their work provided David Marr with an effective algorithm for numerical image processing using wavelets in the early 1980s. This work was very influential in computational neuroscience area.

1960-1980

Between 1960 and 1980, the mathematicians Guido Weiss and Ronald R. Coifman studied the simplest elements of a function space, called *atoms*, with the goal of finding the atoms for a common function and finding the "assembly rules" that allow the reconstruction of all the elements of the function space using these atoms. In 1980, Grossman and Morlet, a physicist and an engineer, broadly defined wavelets in the context of quantum physics. These two researchers provided a way of thinking for wavelets based on physical intuition.

Post-1980

In 1985, Stephane Mallat gave wavelets an additional jump-start through his work in digital signal processing. He discovered some relationships between quadrature mirror filters, pyramid algorithms, and orthonormal wavelet bases. Inspired in part by these results, Y. Meyer constructed the first non-trivial wavelets. Unlike the Haar wavelets, the Meyer wavelets are continuously differentiable; however they do not have compact support. A couple of years later, Ingrid Daubechies used Mallat's work to construct a set of wavelet orthonormal basis functions which perhaps become the cornerstone of wavelet applications today.

2.2 Continuous Wavelet Transform

By using different scaling factors we can stretch or compress the wavelet accordingly, and by changing translation parameter we can cause delay or hastening to the wavelet position in time. The Continuous Wavelet Transform (CWT) is defined as a sum of a signal multiplied by scaled and shifted version of wavelet basis function.

The value of translation parameter affects only the location of the wavelet and has no influence on wavelet duration or bandwidth. For increasing scale, wavelet becomes more dilated and considers the long time/low frequency behavior of the input signal while for the decreasing scale wavelet becomes more compressed and considers short time/high frequency behavior of the input signal. Therefore the scale parameter is inversely proportional to frequency, i.e. low scales correspond to high frequencies and high scales correspond to low frequencies.

The equation of CWT is given in (3), where an input function $f(t)$ is decomposed into a set of wavelet coefficients $\gamma(\kappa, \chi)$. The complex conjugate of the wavelet is given by ψ^* . The parameters κ and χ denote scale and translation respectively, and they represent new dimensions of the wavelet transform.

$$\gamma(\kappa, \chi) = \int_{-\infty}^{\infty} f(t) \psi_{\kappa, \chi}^*(t) dt \quad (2.3)$$

The wavelets functions used in (2.3) are generated using single mother wavelet by changing the scaling parameter and translating the wavelet along the time axes by amount of χ :

$$\psi_{\kappa, \chi}(t) = \frac{1}{\sqrt{\kappa}} \psi\left(\frac{t - \chi}{\kappa}\right) \quad (2.4)$$

As majority of the transforms, CWT is also reversible. Under suitable assumptions about $f(t)$ and ψ , the original signal can be reconstructed from wavelet coefficients by applying the formula for inverse wavelet transform:

$$f(t) = \frac{1}{c_\psi} \int_{\kappa} \int_{\chi} \gamma(\kappa, \chi) \frac{1}{\kappa^2} \psi\left(\frac{t - \chi}{\kappa}\right) d\chi d\kappa \quad (2.5)$$

where $c_\psi = \int_{\mathbb{R}} \frac{|\hat{\psi}(\omega)|^2}{|\omega|} d\omega$ and $\hat{\psi}(\omega)$ denotes the Fourier transform of $\psi(\omega)$.

2.3 Discrete Wavelet Transform

The CWT is less useful for practical problems because the wavelet coefficients are highly redundant to be found and they have to be calculated analytically. Moreover, the calculation of the wavelet transform can take a lot of time and computational power. Therefore the discrete wavelets are more practical to use.

As the name already indicates the discrete wavelets does not use continuously scalable and translatable wavelets but ones that are scaled and translated in discrete steps. The equation for mother wavelet (2.4) can be rewritten for discrete scale and translation as:

$$\psi_{\alpha, \beta}(t) = \sqrt{\kappa_0^\alpha} \psi(\kappa_0^\alpha t - \beta \chi_0) \quad (2.6)$$

In equation (2.6) κ_0 stands for fixed dilation step and χ_0 is translation factor. The integers α and β denote scale and translation indices respectively. The most natural choice for dilation step is 2 as this result in octave bands, also known as dyadic scales. In this case for each subsequent value of scale index, wavelet is compressed in frequency domain by a factor 2 and consequently stretched in time domain by the same factor. The translation factor is usually set to 1 in order to get dyadic sampling of the time axes as well.

The output of wavelet transform when discrete wavelets are utilized would be series of wavelet coefficients:

$$\gamma(\alpha, \beta) = \int_{-\infty}^{\infty} f(t) \psi_{\alpha, \beta}^*(t) dt \quad (2.7)$$

In order to reconstruct the original signal from wavelet coefficients following condition should be satisfied [2].

$$A \|f\|^2 \leq \sum_{\alpha} \sum_{\beta} |\langle f, \psi_{\alpha, \beta} \rangle|^2 \leq B \|f\|^2 \quad (2.8)$$

Equation (2.8) indicates that the energy of the wavelet coefficients should be bounded by two positive bounds ($A > 0$) and ($B < \infty$) where $\|f\|^2$ denotes the energy of input signal $f(t)$.

The wavelets functions $\psi_{\alpha, \beta}(t)$ with $\alpha, \beta \in \mathbb{Z}$ should form a frame bounded by A and B . If the bound A is not equal to the bound B the decomposition wavelet differs from the reconstruction wavelet and we speak of a dual frame. More favorable situation is obtained for so-called tight frame where two bounds are equal to each other. Furthermore if $A = B = 1$ the tight frame becomes an orthogonal basis.

The basis function of a wavelet is called orthogonal if the wavelets generated by dilations and translations are orthogonal to each other, i.e.:

$$\int \psi_{\alpha, \beta}(t) \psi_{p, r}^*(t) dt = \begin{cases} 1 & \text{if } \alpha = p \text{ and } \beta = r \\ 0 & \text{otherwise} \end{cases} \quad (2.9)$$

In the rest of this chapter we will consider in general orthonormal wavelets. The reconstruction of original signal for orthonormal wavelet basis function can be simply obtained by:

$$f(t) = \sum_{\alpha} \sum_{\beta} \gamma(\alpha, \beta) \psi_{\alpha, \beta}(t) \quad (2.10)$$

2.4 Multiresolution Analysis

The Multi resolution analysis (MRA) uses a scaling function to create a series of approximations of a signal or image, each differing by a factor of 2 from its nearest neighboring approximation. Wavelet functions are then used to encode the difference (detail) in information between adjacent approximations. MRA defines a set of requirements for the scaling functions. Given a scaling function that meets these requirements we define a wavelet function to use.

The complete representation of a signal $f(t)$ requires an infinite number of wavelet functions $\psi_{\alpha,\beta}(t)$, as each following wavelet at increased scale covers only a part of the remaining spectrum. This can be overcome by introducing a low-pass complementary function $\varphi(t)$, called scaling function. The extended scaling functions are generated by time shifted version of a single basis scaling function, i.e.:

$$\varphi_{\alpha,\beta}(t) = 2^{\alpha/2} \varphi(2^\alpha t - \beta) \quad \beta \in \mathbb{Z} \quad \varphi \in L^2 \quad (2.11)$$

L^2 in equation (2.11) implies that the integral of the square of the modulus is well defined.

MRA describes the construction of orthonormal wavelets using family of subspaces that has to satisfy certain properties. The closed subspaces spanned by the scaling functions over integers $-\infty < \beta < \infty$ are defined by:

$$V_\alpha = \overline{\underset{\beta}{Span}\{\varphi_\beta(2^\alpha t)\}} = \overline{\underset{\beta}{Span}\{\varphi_{\alpha,\beta}(t)\}} \quad (2.12)$$

The low values of α represent coarse detail of a signal while higher values of α represent the finer detail. MRA requires the spanned spaces by scaling functions V_α to have finite energy and that they are ordered by inclusion as $0 \dots \subset V_{-2} \subset V_{-1} \subset V_0 \subset V_1 \subset V_2 \dots L^2$ [8], i.e.:

$$V_\alpha \subset V_{\alpha+1} \quad \forall \alpha \in \mathbb{Z}, \quad \bigcap_{\alpha \in \mathbb{Z}} V_\alpha = \{0\}, \quad \text{and} \quad \bigcup_{\alpha \in \mathbb{Z}} V_\alpha = L^2(\mathbb{R}) \quad (2.13)$$

According to equation (2.13) the space that contains high resolution signal will also contain information about lower resolution of the signal, for example V_2 contains V_1 which contains V_0 et cetera. The nested vector spaces spanned by the scaling functions are illustrated in figure 2-1.

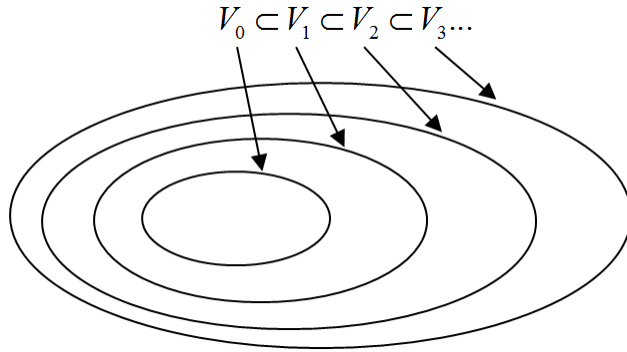


Figure 2-1 : Spaces Spanned by the Scaling Functions

We can express scaling function $\varphi(t)$ which span V_0 as a weighted sum of shifted $\varphi(2t)$ which span V_1 using refinement equation:

$$\varphi(t) = \sum_n h(n) \sqrt{2} \varphi(2t - n), \quad n \in \mathbb{Z} \quad (2.14)$$

In (2.14) $h(n)$ denotes the scaling function coefficients. This equation shows that scaling function can be constructed by the sum of its half-length translations.

The wavelets in MRA are defined as orthogonal bases that span the differences between the spaces spanned by the scaling functions at various scales. Let the subspace spanned by the wavelet be W_{j-1} then spans V_1 and V_2 can be written as:

$$\begin{aligned} V_1 &= V_0 \oplus W_0 \\ V_2 &= V_1 \oplus W_1 = (V_0 \oplus W_0) \oplus W_1 \\ &\vdots \\ V_{\alpha+1} &= V_\alpha \oplus W_\alpha = \bigoplus_{l=0}^{\alpha} W_l \quad \forall \alpha \in \mathbb{Z} \end{aligned} \quad (2.15)$$

Nested vector spaces spanned by the scaling function and wavelet vector spaces are illustrated in figure 2-2.

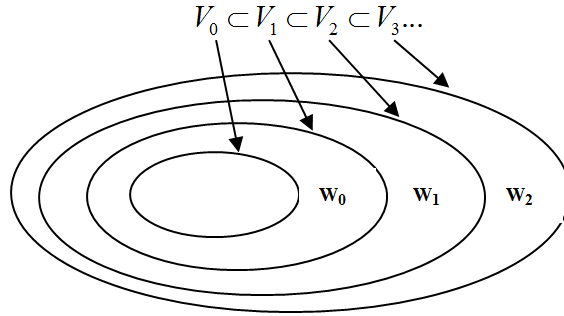


Figure 2-2 : Spaces Spanned by the Scaling Functions and Wavelets

The space W_0 spanned by a wavelet is actually a subspace of V_1 or $W_0 \subset V_1$ mathematically. Therefore, similarly to equation (2.14) the wavelet functions can also be represented by a weighted sum of shifted scaling function $\varphi(2t)$.

$$\psi(t) = \sum_n g(n) \sqrt{2} \varphi(2t - n), \quad n \in \mathbb{Z} \quad (2.16)$$

In (2.16) $g(n)$ denotes the wavelet function coefficients. Because of the orthogonality condition $V_0 \perp W_0 \perp W_1 \perp \dots \perp W_\alpha$ the scaling and wavelet coefficients are related to each other by:

$$g(n) = (-1)^n h(L - 1 - n), \quad \text{for } |h(n)| = L \quad (2.17)$$

The reconstruction formulae for DWT using finite resolution of wavelet and scaling function can now be expressed as [9]:

$$f(t) = \underbrace{\sum_{\beta=-\infty}^{\infty} \lambda(\alpha_0, \beta) 2^{\alpha_0/2} \varphi(2^{\alpha_0} t - \beta)}_{V_{\alpha_0}} + \underbrace{\sum_{\alpha=\alpha_0}^{\infty} \sum_{\beta=-\infty}^{\infty} \gamma(\alpha, \beta) 2^{\alpha/2} \psi(2^\alpha t - \beta)}_{\subset W_\alpha} \quad (2.18)$$

The parameter α_0 in (2.18) sets the coarsest scale which is spanned by the scaling function. The rest is spanned by the wavelets which provide the higher resolution details of the signal. Provided that a wavelet system is orthogonal, the discrete wavelet transform (DWT) coefficients, which are $\lambda(\alpha, \beta)$ and $\gamma(\alpha, \beta)$, can now be defined as equation (2.19) and equation (2.20) respectively:

$$\lambda(\alpha, \beta) = \langle f(t), \varphi_{\alpha, \beta}(t) \rangle = \int f(t) 2^{\alpha/2} \varphi(2^\alpha t - \beta) dt \quad (2.19)$$

$$\gamma(\alpha, \beta) = \langle f(t), \psi_{\alpha, \beta}(t) \rangle = \int f(t) 2^{\alpha/2} \psi(2^\alpha t - \beta) dt \quad (2.20)$$

2.5 Filter Banks

The discrete wavelet transform can be efficiently represented by filtering operations. The weights $h(n)$ given by scaling function coefficients in (2.14) can be represented by low-pass filter H . Similarly the weights of wavelet function $g(n)$ corresponds to high-pass filter G . Therefore the equations (2.14) and (2.16) can be viewed as discrete time filtering with filters H and G respectively [3]. In the rest of this thesis we will refer to filter H as **scaling filter** and to filter G as **wavelet filter**. Filtering a signal can be viewed as the convolution of signal with filter's coefficients. For a Finite Impulse Response (FIR) filter H of length L and an input signal $x(n)$ the filtering operation is given by:

$$x(n) * h(n) = \sum_{k=0}^{L-1} x(k)h(n-k) \quad (2.21)$$

Due to orthogonality condition wavelet and scaling filter are related to each other according to equation (2.17). In frequency domain the spectrum of wavelet filter can be seen as the mirror image at frequency of $\pi/2$ of scaling filter's spectrum. The scaling filter is actually half band Low-Pass Filter (LPF) and complementary wavelet filter is half band High-Pass Filter (HPF). The frequency response of these orthogonal filters is depicted in figure 3.

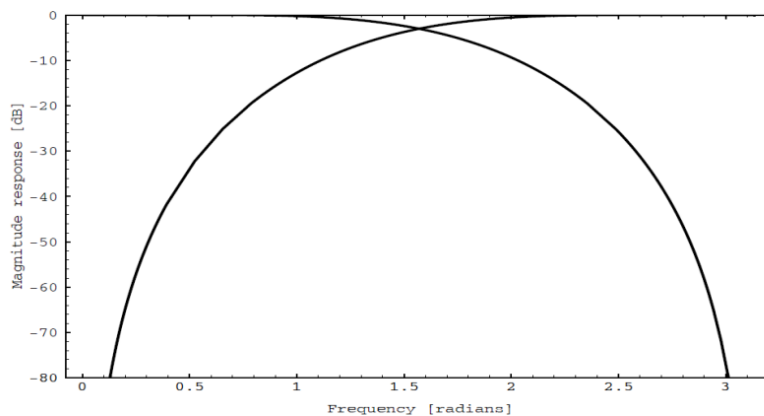


Figure 2-3 : Frequency response using Daubechies filter with length 8

Filtering of a signal with perfect half band pass filter removes exactly half of the frequency components from the input signal meaning that the number of samples in the filtered signal has now became redundant. In order to remove redundancy we can perform down-sampling. For half band pass filter the filtered signal should be down-sampled by 2 in order to remove redundant information. If the signal is down-sampled by a larger factor we will lose information and the frequency components will be mixed up. The down-sampling by factor 2 can be seen as taking every other sample of the input signal and discarding the rest of the samples, i.e.:

$$y(n) = x(2n) \quad (2.22)$$

The opposite operation to down-sampling is up-sampling. Up-sampling increases the length of a signal by inserting zeros between each pair of samples. In contrast to down-sampling, up-sampling does not discard information and therefore it can always be inverted.

The up-sampling by a factor 2, doubles the number of samples in a signal by inserting one zero between each pair of samples. This can be mathematically illustrated by:

$$y(m) = \begin{cases} x\left(\frac{m}{2}\right) & \text{for } m = 2n \\ 0 & \text{otherwise} \end{cases} \quad (2.23)$$

2.5.1 Analysis Filter Bank

The refinement equations given in (2.14) and (2.16) can be rewritten so that the lower scale representations of the wavelet and scaling functions can be expressed in those of higher scale as [5]:

$$\begin{aligned} \varphi(2^\alpha t - \beta) &= \sum_n h(n) \sqrt{2} \varphi(2(2^\alpha t - \beta) - n) \\ &= \sum_n h(n) \sqrt{2} \varphi(2^{\alpha+1} t - 2\beta - n) \\ &= \sum_{m=2\beta+n} h(m-2\beta) \sqrt{2} \varphi(2^{\alpha+1} t - m) \end{aligned} \quad (2.24)$$

$$\begin{aligned} \psi(2^\alpha t - \beta) &= \sum_n g(n) \sqrt{2} \psi(2(2^\alpha t - \beta) - n) \\ &= \sum_n g(n) \sqrt{2} \psi(2^{\alpha+1} t - 2\beta - n) \\ &= \sum_{m=2\beta+n} g(m-2\beta) \sqrt{2} \psi(2^{\alpha+1} t - m) \end{aligned} \quad (2.25)$$

Using derivation carried above for wavelet and scaling function, we can express similarly DWT coefficients at scale α by coefficients at the higher scale $\alpha+1$ as follows:

$$\begin{aligned}
\lambda(\alpha, \beta) &= \langle f(t), \varphi_{\alpha, \beta}(t) \rangle \\
&= \int f(t) 2^{\alpha/2} \varphi(2^\alpha t - \beta) dt \\
&= \sum_m h(m - 2\beta) \int f(t) 2^{\alpha+1/2} \varphi(2^{\alpha+1} t - m) dt \\
&= \sum_m h(m - 2\beta) \lambda(\alpha + 1, m)
\end{aligned} \tag{2.26}$$

$$\begin{aligned}
\gamma(\alpha, \beta) &= \langle f(t), \psi_{\alpha, \beta}(t) \rangle \\
&= \int f(t) 2^{\alpha/2} \psi(2^\alpha t - \beta) dt \\
&= \sum_m g(m - 2\beta) \int f(t) 2^{\alpha+1/2} \psi(2^{\alpha+1} t - m) dt \\
&= \sum_m g(m - 2\beta) \gamma(\alpha + 1, m)
\end{aligned} \tag{2.27}$$

Equations (2.26) and (2.27) imply that wavelet and scaling DWT coefficients at the certain scale can be calculated by taking a weighted sum of DWT coefficients from higher scales. This can be viewed as convolution between the DWT coefficients at scale $\alpha + 1$ with wavelet and scaling filter coefficients and subsequently down-sampling each output with factor 2 to obtain new wavelet and scaling DWT coefficients at scale α . Therefore, we can describe equations (2.26) and (2.27) by a 2-channel filter bank illustrated in figure 2-4.

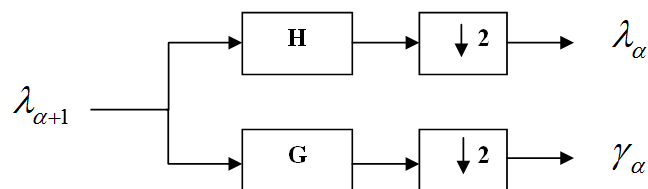


Figure 2-4 : Analysis Filter Bank

The 2-channel filter bank first splits the input signal in two parts and filters one part with filter H and other with filter G . Both filtered signals are then down-sampled by 2 and resulting signals are forwarded to the output of the 2-channel filter bank. Each output signal will therefore contain half the number of samples and will span half of the frequency band compared to the input signal. It should be noticed that the number of samples at the input of the filter bank equals the number of samples at the output.

The complete representation of the DWT can be obtained by iteration of the 2-channel filter bank and taking repeatedly scaling DWT coefficients λ as input. The iteration process starts with λ at the largest scale which is equal to the original signal. The number of stages in iteration process will determine the DWT resolution and therefore the number of channels. If the input signal f has 512 samples and contains frequencies that lie between 0 and π , the first stage of filter banks will divide the input signal into 256 samples in each branches after down-sampling. The second stage filter banks will repeat the same process to the previous output and so on. The resulting decompositions together will still contain 512 samples and span the same frequency band as the original signal but they are decomposed in different DWT coefficients. The subband structure of wavelet decomposition in frequency domain can be calculated using Fourier transformation.

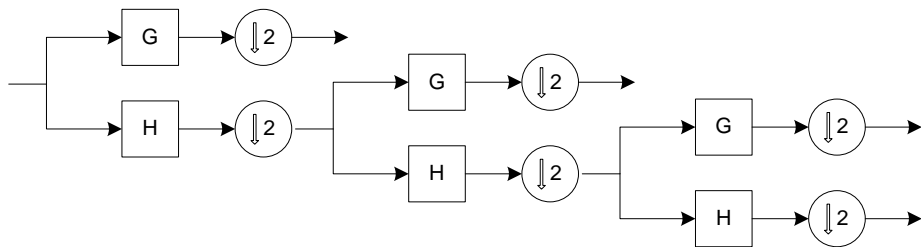


Figure 2-5 : 3-Stage Analysis Filter Banks

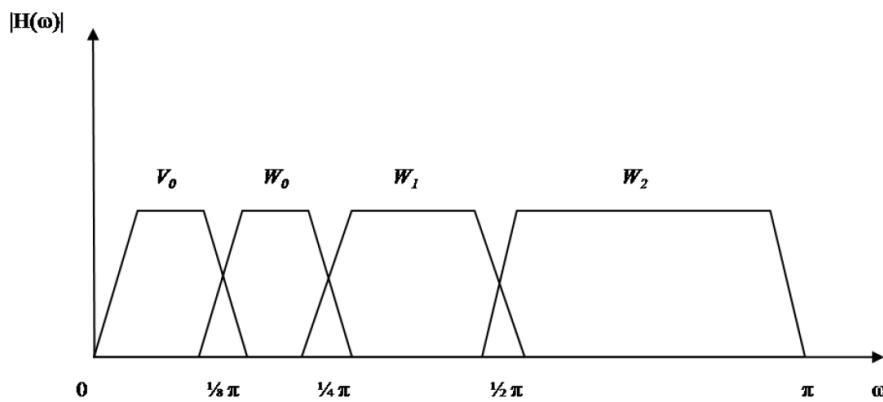


Figure 2-6 : Frequency Bands for 3-Stage Analysis Filter Banks

2.5.2 Synthesis Filter Bank

The reconstruction formula for DWT is given in equation (2.18). If we now substitute the refinement equations for wavelet and scaling function, (2.16) and (2.14) respectively, into reconstruction equation (2.18) we get:

$$\begin{aligned} f(t) = & \sum_{\beta} \lambda(\alpha, \beta) \sum_n h(n) 2^{\frac{(\alpha+1)}{2}} \varphi(2^{\alpha+1}t - 2\beta - n) \\ & + \sum_{\beta} \gamma(\alpha, \beta) \sum_n g(n) 2^{\frac{(\alpha+1)}{2}} \varphi(2^{\alpha+1}t - 2\beta - n) \end{aligned} \quad (2.28)$$

Multiplying both side of this equation with $\varphi(2^{\alpha+1}t - \beta')$ and taking integrals allows us to describe the DWT coefficients at higher scales by those of the lower scale as [5]:

$$\lambda(\alpha+1, \beta) = \sum_m \lambda(\alpha, m) h(\beta - 2m) + \sum_m \gamma(\alpha, m) g(\beta - 2m) \quad (2.29)$$

The equation (2.29) implies that the DWT coefficients at certain scale level α can be reconstructed by taking a combination of weighted wavelet and scaling DWT coefficients at previous scale α . This process can be described by the 2-channel synthesis filter bank, illustrated in figure 2-7.

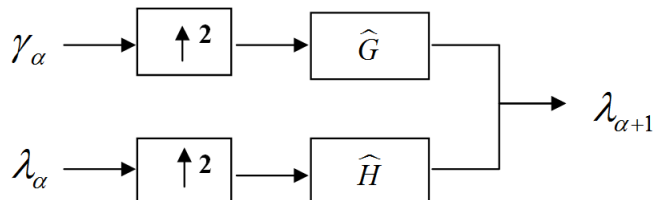


Figure 2-7 : Synthesis Filter Bank

The 2-channel synthesis filter bank performs exactly opposite operation compared to previously discussed analysis filter bank. The wavelet and scaling DWT coefficients are first up-sampled by factor 2 and after that the wavelet function DWT coefficients are filtered with HPF G while scaling function DWT coefficients are filtered with LPF H . The two filtered signals are then added to each other to construct DWT coefficients at higher scale. The filters H and G are according to equation (2.28) and equations (2.25) and (2.26) time reversed version of filters H and G respectively.

The decomposition of a signal in terms of coefficients is called discrete wavelet transform. In order to reconstruct the original signal from coefficients we can apply inverse wavelet transform, abbreviated

IDWT. The IDWT can be efficiently implemented by iterating the 2-channel synthesis filter bank in the same manner like we have done in the previous paragraph for the 2-channel analysis filter bank. The example of 3-stages synthesis tree is illustrated in figure 2-8.

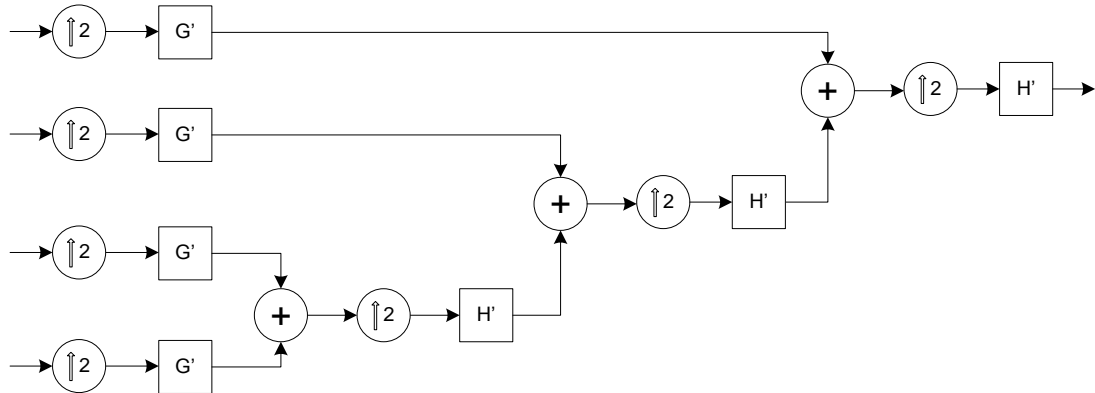


Figure 2-8 : 3-Stage Synthesis Filter Banks

If our primal assumption of orthogonality in equation (2.17) is valid, the reconstructed signal then is simply a delayed version of the input signal ($x(n) = y(n)$). The filter banks that satisfy this property are called **perfect reconstruction filter banks**.

2.6 Wavelet Packets

The resolution of discrete wavelet transform, as described so far, depends on the frequency bands. Because we are iterating the 2-channel filter bank only for the low pass output (scaling function branch), at the end of decomposition the high frequencies will have wide bandwidths while low frequencies will have narrow bandwidths, as seen in figure 2-6.

The wavelet packet transform on the contrary performs the iteration of the 2-channel filter bank on both sides: low pass (scaling function branch) and high pass (wavelet function branch). Because the high frequencies are decomposed in the same manner as low frequencies the wavelet packet transform has evenly spaced frequency resolution. Figure 2-9 shows the frequency bands for 3-stage wavelet packet tree.

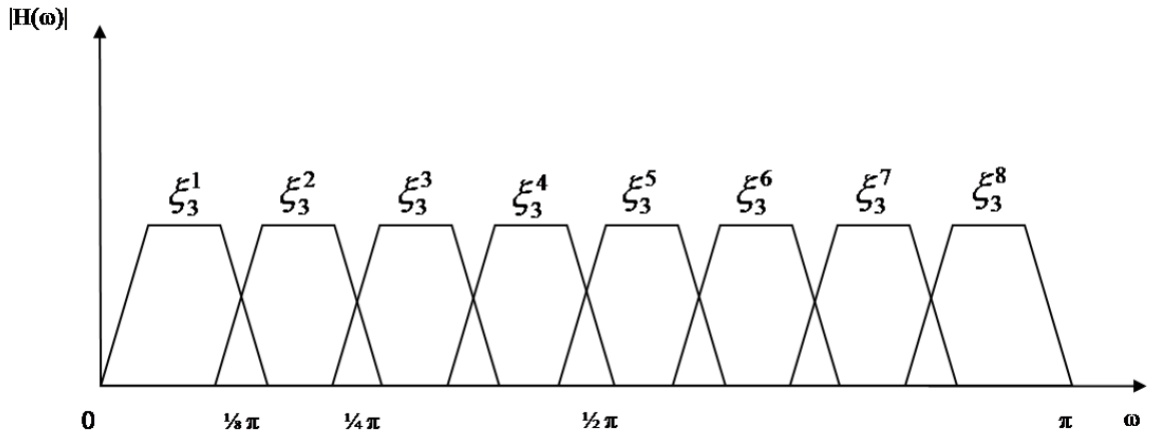


Figure 2-9 : Frequency Bands for 3-Stage Wavelet Packets Tree

The filter bank structure for wavelet packet transform expands to a full binary tree. In order to make clear distinction between different sets of coefficients we will label each wavelet packet ξ by the level l which corresponds to the depth of the node in the tree and by the current position p of the node at a given level.

Wavelet packet decomposition recursively splits each parent node in two orthogonal subspaces W_l^p located at the next level:

$$W_l^p = W_{l+1}^{2p} \oplus W_{l+1}^{2p+1} \quad (2.30)$$

The subspaces given in equation (2.30) are those spanned by the basis functions of wavelet packets:

$$W_l^p = \overline{\text{Span} \{ 2^{l/2} \xi_l^p (2^l t - \beta) \}} \quad (2.31)$$

Wavelet packet coefficients ξ at a certain level are calculated by convolving the wavelet and scaling filter with wavelet packets coefficients from previous level. This action is performed repeatedly for all wavelet packets until the full binary tree is obtain with desired depth. The equation (2.30) shows the recursive equation for wavelet packets generation. The wavelet packets coefficients $\xi_{l+1}^{2p}(\beta)$ are generated using the scaling filter and coefficients $\xi_l^{2p+1}(\beta)$ are created using the wavelet filter.

$$\xi_{l+1}^{2p}(\beta) = \sum_m h(m - 2\beta) \xi_l^p(m) \quad (2.32)$$

$$\xi_{l+1}^{2p+1}(\beta) = \sum_m g(m - 2\beta) \xi_l^p(m)$$

In the regular DWT decomposition for each additional level we need only to perform single iteration of 2-channel filter bank while in wavelet packet transform the number of iterations is exponentially proportional to the number of levels. Therefore, the wavelet packet transform has higher computational complexity when compared to regular DWT. By utilization of fast filter bank algorithm wavelet packet transform requires $O(N \log(N))$ operation, similar to FFT while DWT needs only $O(N)$ calculation [10]. Figure 2-10 and 2-11 illustrates the full binary tree for the 3-stages wavelet packet analysis and synthesis, respectively.

The reconstruction of wavelet packets is also performed in an iterative method. For each pair of wavelet packets coefficients at level l of the tree we can calculate wavelet packets coefficients at the previous level $l-1$ by:

$$\zeta_l^p(\beta) = \sum_m \zeta_{l+1}^{2p}(m) h(\beta - 2m) + \sum_m \zeta_{l+1}^{2p+1}(m) g(\beta - 2m) \quad (2.33)$$

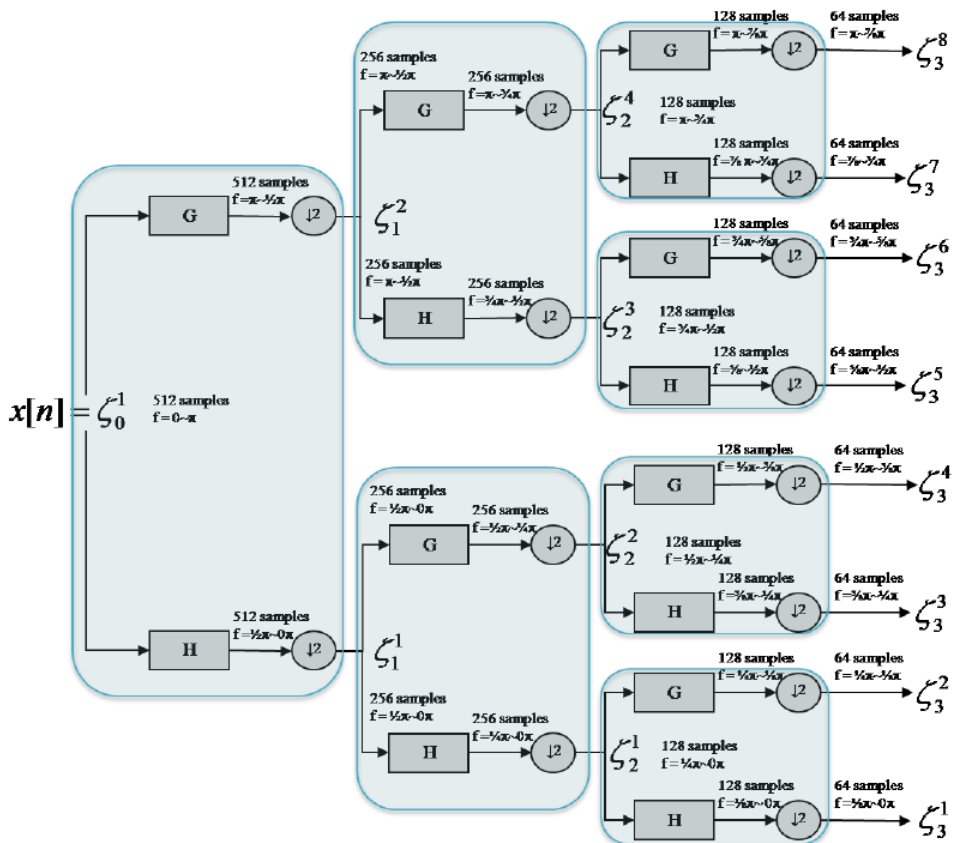


Figure 2-10 : 3-Stage Wavelet Packets Analysis Tree [11]

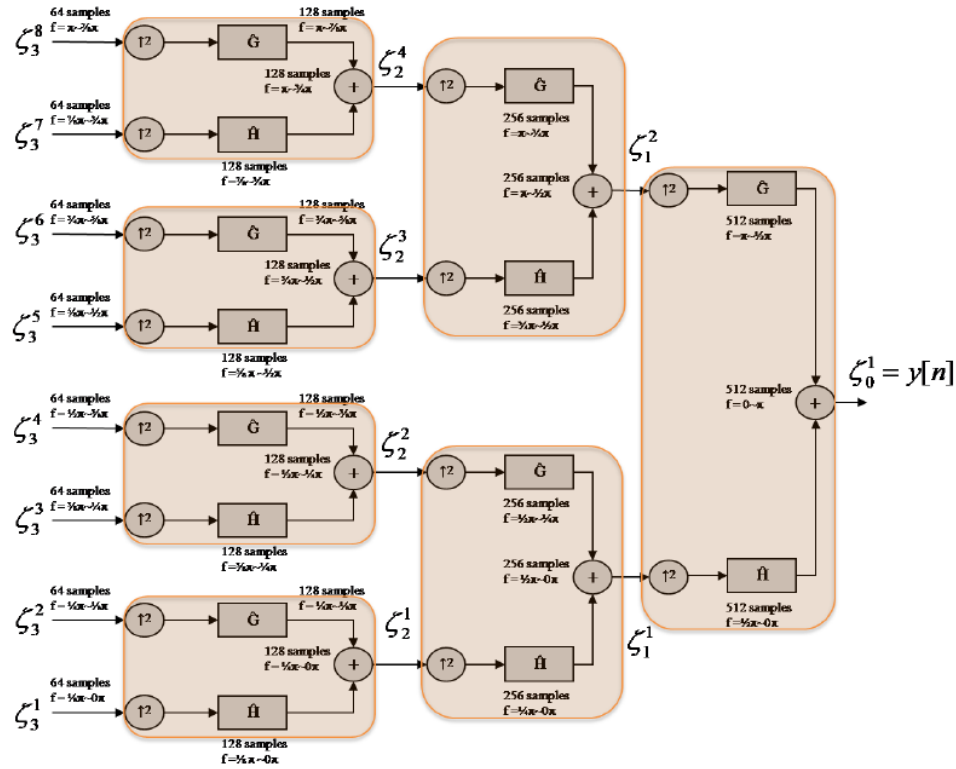


Figure 2-11 : 3-Stage Wavelet Packets Synthesis Tree [11]

2.6.1 Wavelets Families

Each wavelet has some distinguishing characteristics that make it more suitable for one application than other. Therefore during design of a system the careful consideration of different wavelet properties should be made with respect to the system requirements. The selection of wavelets is generally made on certain wavelet properties, such as: Compact Support, Orthogonality, Symmetry, and K -Regularity/Vanishing Moments.

Compact support is defined by the length of the filter. In order to decrease computational complexity we prefer shorter filters however, filter length is closely related to other wavelet properties like orthogonality or regularity. This means by setting other wavelet properties we automatically define minimum filter length.

Orthogonality ensures perfect reconstruction making it one of the most vital wavelet properties. For communication purposes we absolutely require orthogonal wavelets but for other applications orthogonality is occasionally too restrictive.

Symmetrical wavelets have as feature that transform of the mirror of an image is the same to the mirror of the wavelet transform. None of the orthogonal wavelets except Haar wavelet is symmetric. Although, requiring symmetric wavelets involuntarily means that wavelets are not orthogonal there

are some applications that prefer symmetric wavelets above orthogonal ones. For instance image compression techniques like JPEG2000 uses biorthogonal symmetric wavelets. Because by compression of an image we discard one part of the wavelet coefficients containing high detail, the perfect reconstruction has become impossible anyhow. The fulfillment of symmetry property in JPEG2000 on the other hand results in more natural, smooth images.

K-regularity is also an important measure for wavelets because it helps reduce the number of non-zero coefficients in the high-pass sub-bands and it is one of the easiest ways to determine if a scaling function is fractal. Usually the more a wavelet has zero wavelet moments the smoother the scaling function is. However this is not a tight condition. The smoothness is actually defined by the continuous differentiability of the scaling function. There are two ways in which smoothness can be defined: local by the Hölder measure and global by the Sobolev measure [11].

The following are some of the popular wavelets and their general properties [12]:

Haar Wavelets: Compactly supported wavelet, the oldest and the simplest wavelet.

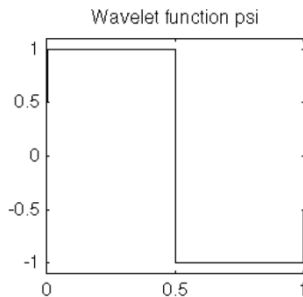
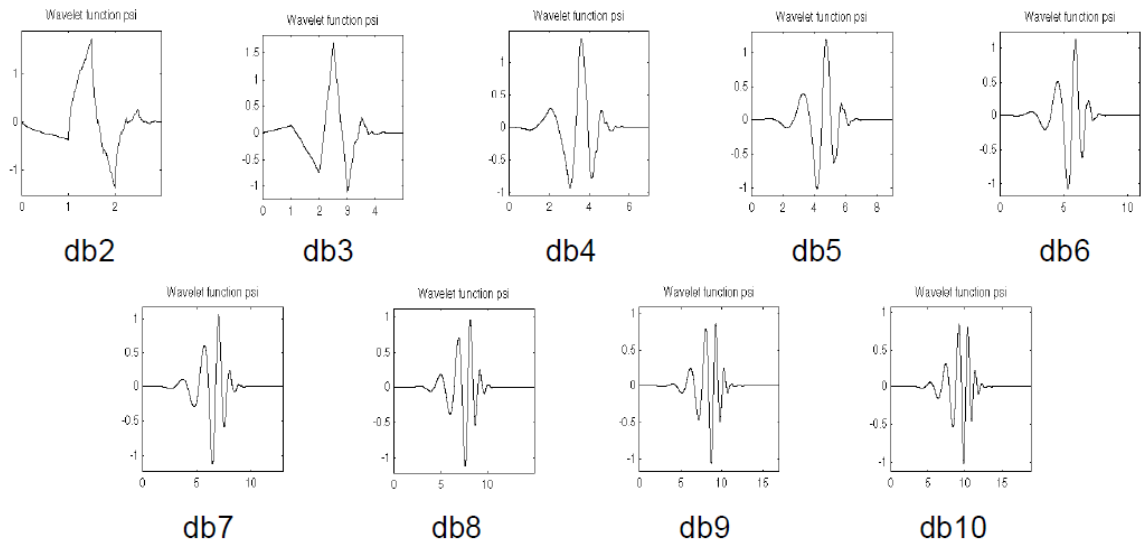
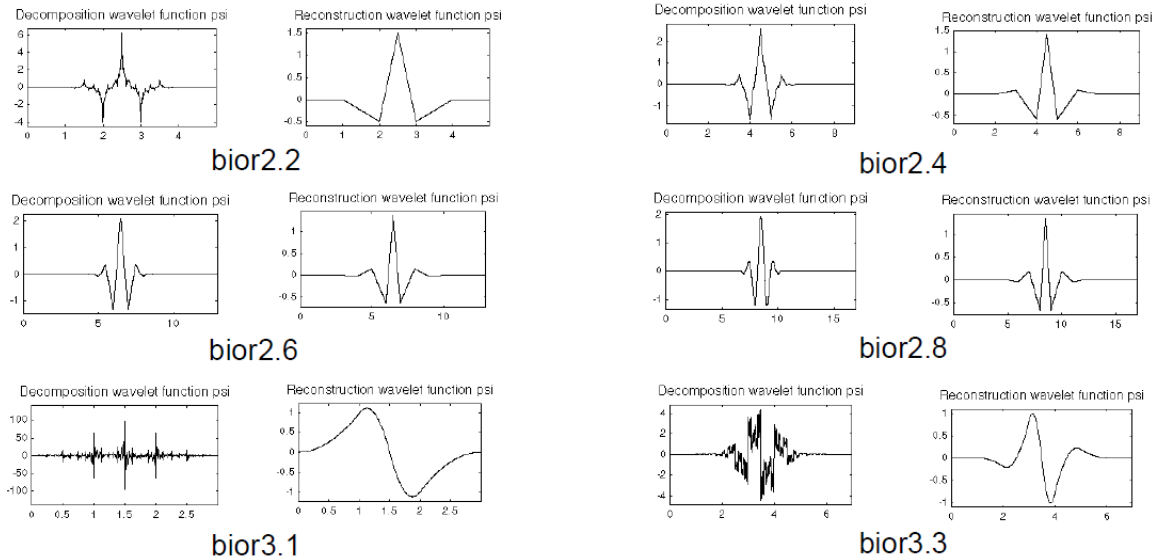


Figure 2-12 : Haar Wavelets

Daubechies Wavelets: Compactly supported wavelets with extremal phase and highest number of vanishing moments for a given support width. Associated scaling filters are minimum-phase filters.

**Figure 2-13 : Daubechies Wavelets**

Biorthogonal Wavelets: Compactly supported biorthogonal spline wavelets for which symmetry and exact reconstruction are possible with FIR filters (in orthogonal case it is impossible except for Haar).

**Figure 2-14 : Biorthogonal Wavelets**

Coiflets Wavelets: Compactly supported wavelets with highest number of vanishing moments for both φ and ψ for a given support width.

[Wavelet Theory]

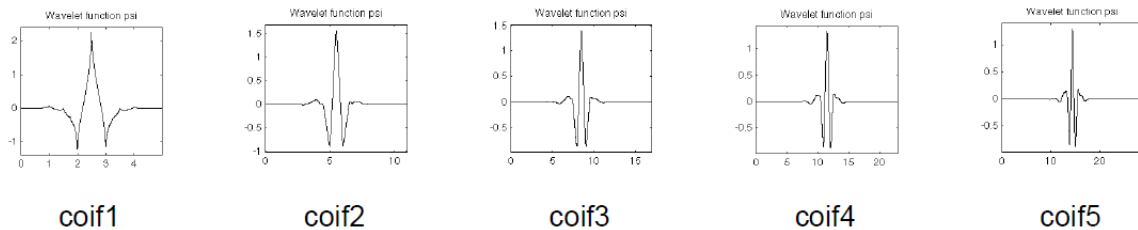


Figure 2-15 : Coiflets Wavelets

Symlets Wavelets: Compactly supported wavelets with least asymmetry and highest number of vanishing moments for a given support width. Associated scaling filters are near linear-phase filters.

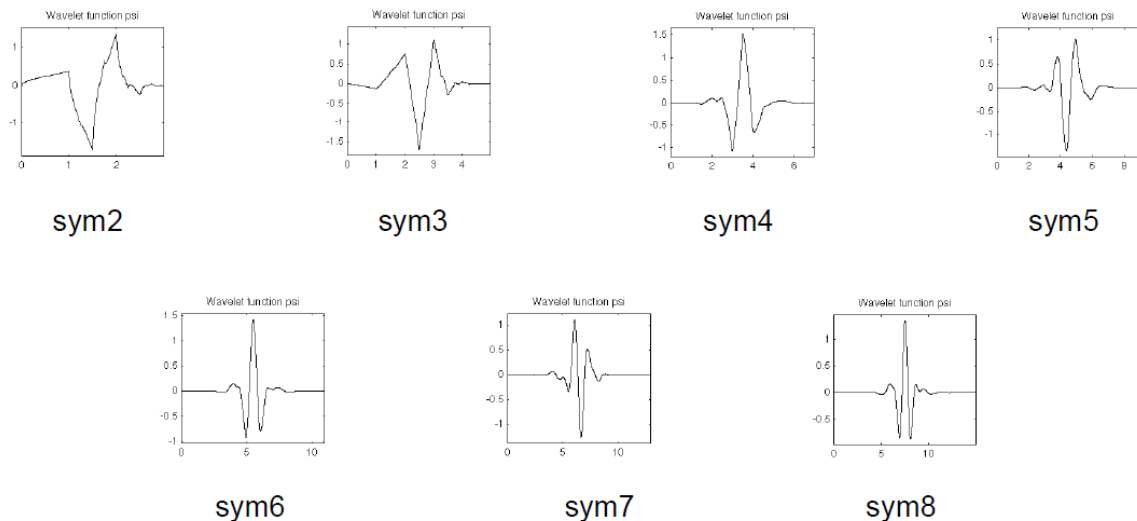


Figure 2-16 : Symlets Wavelets

It can be seen that each wavelet has some distinguishing characteristics that make it more suitable for one application than other. The differences these wavelet properties is summarized in Table 2.1. The **Nr** and **Nd** notations for biorthogonal wavelet are the length of reconstruction scaling filter and length of decomposition scaling filter, respectively.

Table 2-1 : Wavelet Families Properties

Family Name	Haar	Daubechies	Biorthogonal	Coiflets	Symlets
Order N	-	N strictly positive	Various Nr and Nd	N = 1, 2, ..., 5	N = 2, 3, ...
Orthogonal	yes	yes	no	yes	yes
Biorthogonal	yes	yes	yes	yes	yes
Compact	yes	yes	yes	yes	yes
Support					
DWT	possible	possible	possible	possible	possible
CWT	possible	possible	possible	possible	possible
Support	1	2N-1	2Nr+1 for rec., 2Nd+1 for dec.	6N-1	2N-1
Width					
Filters Length	2	2N	max(2Nr,2Nd)+2	6N	2N
Regularity	Haar is not continuous	about 0.2 N for large N	for psi rec.: Nr-1 & Nr-2 at knots	-	
Symmetry	yes	far from	yes	near from	near from
φ Vanishing	-	-	-	2N	-
Moments					
ψ Vanishing	1	N	Nr	2N-1	N
Moments					

2.6.2 Wavelet Packet based Multicarrier Modulation

Wavelet Packet based Multi Carrier Modulation (WPM) is a multiplexing method that makes use of orthogonal wavelet packets waveforms to combine a collection of parallel signals into single composite signal. Fundamentally OFDM and WPM have many similarities as both use orthogonal waveforms as subcarriers and they achieve high spectral efficiency by allowing subcarriers' spectra to overlap one another. The adjacent subcarriers do not interfere with each other as long as the orthogonality between subcarriers is preserved.

The difference between OFDM and WPM is the shape of the subcarriers and in way they are created. OFDM makes use of Fourier bases which are static sinusoidal functions while WPM uses wavelets which offer much more flexibility. By utilization of different wavelets in WPM we can get different subcarriers which lead to different transmission system characteristics. Therefore, it is possible in WPM by selection of wavelets to change the bandwidth efficiency, frequency concentration of subcarriers, sensitivity to synchronization errors, PAPR, etc. [8].

WPM employs Inverse Discrete Wavelet Packet Transform (IDWPT) at the transmitter side and Discrete Wavelet Packet Transform (DWPT) at the receiver side, analogous to the IDFT and DFT used by OFDM transceivers. The IDWPT is implemented by wavelet packet synthesis tree which combines different parallel streams into a single signal. This composite signal is afterwards decomposed at the receiver using wavelet packets analysis tree or so called DWPT. The structure where synthesis tree is placed prior the analysis tree is called transmultiplexer [9].

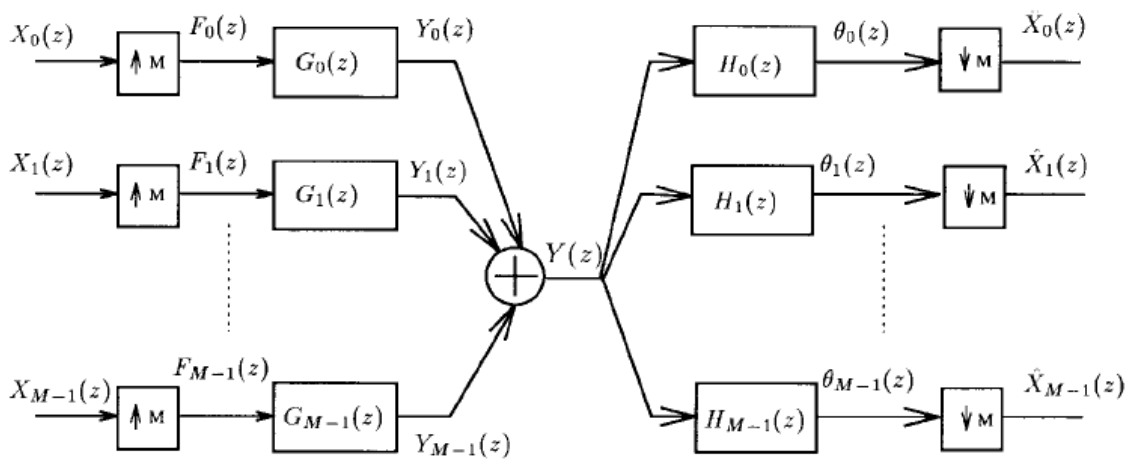


Figure 2-17 : M-band Transmultiplexer structure

The number of levels in synthesis and analysis trees determines the amount of subcarriers in the WPM system by:

$$N = 2^l \quad (2.34)$$

where N determines the number of subcarriers and l represents the number of levels in the filter bank.

The wavelet packet synthesis and analysis tree are constructed by iteration of corresponding 2-channel filter bank, as explained in equation (2.34). Therefore, the subcarriers of WPM are completely determined by the scaling and wavelet filter. The calculation of wavelet packet waveforms is performed in a recursive manner using filters coefficients $h(n)$ and $g(n)$ as:

$$\xi_{l+1}^{2p}(t) = \sqrt{2} \sum_m h(n) \xi_l^p(t - 2^l n) \quad (2.35)$$

$$\zeta_{l+1}^{2p+1}(t) = \sqrt{2} \sum_m g(n) \zeta_l^p(t - 2^l n)$$

The subscripts l in equation (2.35) determines the level in the tree structure and superscript p can be seen as subcarrier index at a given tree depth (level l). The filters in WPM cannot be arbitrary chosen and not all scaling and wavelet filters will fit the requirements for a communication system. First of all, we will only consider FIR filters because they allow wavelet packet transformation to be implemented by described fast recursive algorithm. Furthermore, we require perfect reconstruction and hence the orthogonal subcarriers. These can only be generated by filters that fulfill the orthogonality constraint. The WPM subcarriers are mutually orthogonal if they satisfy the following condition:

$$\langle \zeta_l^p(t), \zeta_l^i(t) \rangle = \sum_k \zeta_l^p(t) \zeta_l^i(t) = \delta(p-i) \quad (2.36)$$

The transmitted signal for WPM is composed of successively modulated WPM symbols that are built from a sum of modulated subcarriers. The WPM transmitted signal in the discrete time domain can be expressed as:

$$S(n) = \sum_u \sum_{k=0}^{N-1} a_{u,k} \zeta_{2^{\log(N)}}^k (n - uN) \quad (2.37)$$

where k denotes the subcarrier index and u denotes the WPM symbol index. The constellation symbol modulating k -th subcarrier in u -th WPM symbol is represented by $a_{u,k}$.

If we assume that the WPM transmitter and receiver are perfectly synchronized and that the channel is ideal, the detected data at the receiver can be given by:

$$\begin{aligned} a_{u',k'} &= \sum_n R(n) \zeta_{2^{\log(N)}}^{k'} (u'N - n) \\ &= \sum_n \sum_u \sum_{k=0}^{N-1} a_{u,k} \zeta_{2^{\log(N)}}^k (n - uN) \zeta_{2^{\log(N)}}^{k'} (u'N - n) \\ &= \sum_n \sum_{k=0}^{N-1} a_{u,k} \left(\sum_n \zeta_{2^{\log(N)}}^k (n - uN) \zeta_{2^{\log(N)}}^{k'} (u'N - n) \right) \\ &= \sum_n \sum_{k=0}^{N-1} a_{u,k} \delta(k - k') \\ &= a_{u,k} \end{aligned} \quad (2.38)$$

In equation (2.38) we have used the fact that different symbols are not interfering with each other and that subcarriers with index other than k are not contributing, according to the orthogonality equation (2.36).

One important property of wavelet based transformation is that the waveforms used in general are longer than the transform duration of one symbol. This cause WPM symbols to overlap in time domain. Thanks to the orthogonality of used waveforms this overlap of the symbols does not automatically lead to Inter Symbol Interference (ISI).

The multicarrier symbols of OFDM are not overlapping each other as IDFT and DFT transform are carried out for each group of subcarriers independently. On the other hand, the use of longer waveforms in WPM allows better frequency localization of subcarriers while in OFDM the rectangular shape of DFT window generates large side lobes. Recall the spectra of WPM and OFDM for 8 subcarriers which are illustrated in chapter 1.

The other non-palatable consequence of time overlap is the inability to use guard interval in WPM systems. Although adding a guard interval severely decreases spectral efficiency, an effective and low complexity method to cope with dispersive channels and time offset. In contrast to the OFDM, in the WPM we will not add cyclic prefix block as it would only lead to the decrease of spectral efficiency without giving any benefits.

2.7 Summary of Wavelet Theory

In this chapter we discussed the history of wavelet, basics of the theory of the wavelet transform, and explained how discrete wavelet transform can be efficiently implemented using filter banks. Due to efficient implementation and the freedom they provide, wavelets have emerged in many different fields. One of the most recent idea is to propose wavelets as a candidate for multicarrier modulation. This is possible because not only wavelet has orthogonal properties like OFDM, which is widely used for multicarrier communication, but wavelet also provide more flexibility than OFDM.

3 SYNCHRONIZATION IMPAIRMENTS

The principle of multicarrier (MC) modulation is to divide the total bandwidth into several parallel narrow subbands, giving multicarrier systems some important advantages, such as increased symbol duration and the use of several narrow subbands, when compared to single-carrier (SC) communication systems. Increased symbol duration means better performance in dispersive channels and by using of several narrow subbands, narrow band interference or strong frequency band attenuation only affects particular subcarriers and not the whole system. Because of these advantages and the fact that wireless systems in the time-dispersive environments (e.g. home, office, etc.) is becoming more and more widely used, MC modulation techniques have gained popularity in the last decades.

One of the biggest problem in wireless transmission system is the presence of time synchronization error. Time synchronization error occurs when the start of the MC symbol is incorrectly detected, selecting part of the adjacent symbol while discarding some samples at begin or at end of the useful symbol. Due to time synchronization errors the Inter Symbol Interference (ISI) arises as well as the Inter Carrier Interference (ICI). The use of guard intervals, like cyclic prefix in OFDM, can significantly improve the system performance in case of timing errors. However, the use of guard interval is not feasible solution for WPM systems because of time-overlapping nature of wavelet packet transform [11].

In case of OFDM, the effects of time synchronization errors are well documented in the literature [13]-[15] and number of synchronization techniques are reported to estimate and reduce the time offset effects [16]-[21].

Besides the synchronization errors in form of time synchronization error, the MC transceiver can also suffer from frequency and phase misalignment. In OFDM and WPM, the subcarriers have to be closely spaced to each other, and overlapping over each other, in order to achieve high efficiency in bandwidth utilization.

Although both OFDM and WPM have orthogonal subcarriers so that even the subcarriers overlap they do not interfere one another, the radio front-end induced impairments as frequency offset and/or phase noise. These impairments can cause the subcarriers to lose their mutual orthogonality and to begin interfering one with another.

Similar to the time offset effects on the performance of the system, also for frequency synchronization errors the documentation is far more comprehensive for OFDM than for WPM. The sensitivity of the OFDM to the frequency synchronization error is reported in [22]-[23] and there are various techniques for OFDM frequency synchronization available in the literature [24]-[25].

In this chapter we will address different types of synchronization errors for the WPM transceiver, and compare the performance of WPM under these errors to OFDM. Each synchronization error will be treated separately. First we will treat the time offset between transmitter and receiver, after which follows the discussion of frequency offset. We will finalize this chapter with summary of the results.

3.1 Time Offset in Multicarrier Modulation

One of the major concerns of a multicarrier system is their vulnerability to timing synchronization errors, which occur when multi-carrier symbols are not perfectly aligned at the receiver. Because of the time offset samples outside a WPM or OFDM symbol get erroneously selected, while useful samples at the beginning or at the end of that particular symbol get discarded.

The time synchronization error is modeled by shifting the received data samples by a time offset value t_ϵ to the left or right, depending on the sign of the t_ϵ . If we assume that transmitted signal is given by $S(n)$, the received signal $R(n)$ in presence of time synchronization error can be expressed as:

$$R(n \pm t_\epsilon(k)) = S(n) + w(n) \quad (3.1)$$

Without loss of generality, we assume for the moment that $w(n) = 0$.

Time offset degrades the performances of multicarrier transceivers for the greatest part by introducing inter-symbol interference (ISI) and inter-carrier interference (ICI). WPM and OFDM share many similarities as both are orthogonal multicarrier systems but in case of timing error there is a major difference that causes different behaviors for each transmission scheme.

The actual length of the WPM symbols is defined by the wavelet used and in general it is significantly longer than the OFDM symbol. This excessive length of WPM symbols does not cause frame size to grow by allowing symbols to overlap one another. In case of time offset this overlap of the symbols in

WPM causes each symbol to interfere with several other symbols while in OFDM each symbol can only interfere with one adjacent symbol.

The second important difference between the two transmission schemas is the use of the guard interval between the symbols. OFDM uses cyclic prefix that significantly improves its performance when time errors occur, assuming that time offset is not exceeding the size of cyclic prefix and that the direction of time shift is towards the cyclic prefix. The WPM, on the other hand, cannot benefit from such guard interval since the WPM symbols overlap one another.

3.1.1 Time Offset in OFDM

Adding a Cyclic prefix is an effective and low complexity method to cope with dispersive channels and time synchronization errors in OFDM transceivers. Two distinct situations can occur under time synchronization errors, depending on the direction of the time offset:

- Time synchronization error away from own cyclic prefix (to the right).
- Time synchronization error towards own cyclic prefix (to the left).

In case of time synchronization error **away** from CP, the FFT window is misaligned to the right. This situation is illustrated by 3 OFDM symbols ($u-1, u, u+1$) in Fig. 3-1. Each OFDM symbol consists of N data samples and an extension of N_{CP} samples representing cyclic prefix. The FFT window in the situation illustrated will contain $N - t_e$ data samples $((t_e + 1), (t_e + 2), \dots, N)$ of the considered u -th OFDM symbol, missing first t_e time offset samples. Instead t_e samples $(1, 2, \dots, t_e)$ of the next $(u + 1)$ -th symbol will be erroneously selected.

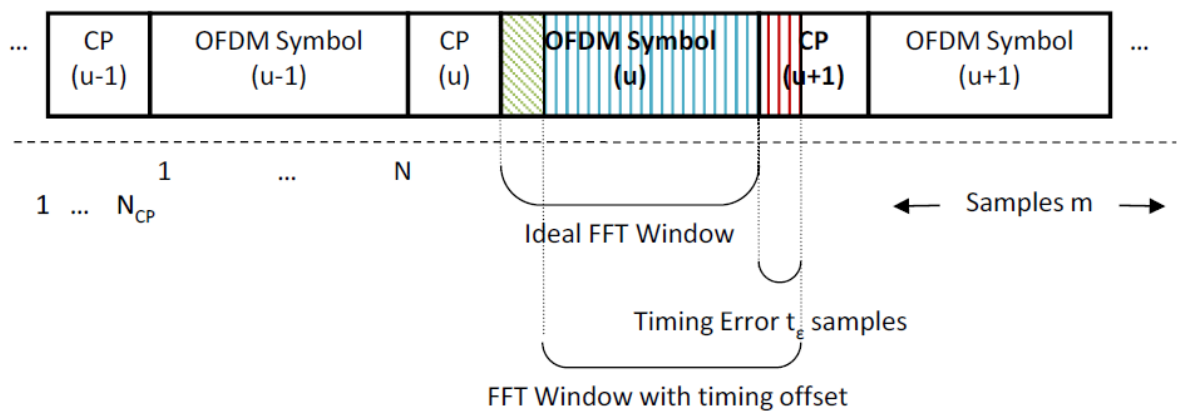


Figure 3-1 : Timing offset away from CP (to the right) [11]

[Synchronization Impairments]

An OFDM system that is affected by timing error and where samples of neighboring symbol are wrongly selected experience severe degradation of the performance. The demodulated OFDM signal after FFT can be written as:

$$\hat{a}_{u',k'} = \underbrace{\frac{N-t_\varepsilon}{N} a_{u',k'} e^{j2\pi \frac{k'}{N} t_\varepsilon}}_{\text{Useful Signal}} + \underbrace{\frac{1}{N} \sum_{n=0}^{N-1-t_\varepsilon} \sum_{k=0; k \neq k'}^{N-1} a_{u',k} e^{j2\pi \frac{k(n+t_\varepsilon)}{N}} e^{-j2\pi \frac{k'n}{N}}}_{\text{ICI}} + \underbrace{\frac{1}{N} \sum_{n=N-t_\varepsilon}^{N-1} \sum_{k=0}^{N-1} a_{u+1,k} e^{j2\pi \frac{k(n-N+t_\varepsilon)}{N}} e^{-j2\pi \frac{k'n}{N}}}_{\text{ISI}} \quad (3.2)$$

The first component of (3.2) represents useful signal which is attenuated and phase shifted by a term proportional to subcarrier index k' . The second component of (1) gives ICI and the third component stands for ISI with next symbol.

In case of time synchronization error **towards** the CP, the FFT window is misaligned to the left, illustrated in Fig. 2. In this case FFT window consists of first $N-t_\varepsilon$ samples ($1, 2, \dots, (N-t_\varepsilon)$) of the considered u th OFDM symbol and the last t_ε samples of the own cyclic prefix. We assume for the convenience that $t_\varepsilon < N_{CP}$.

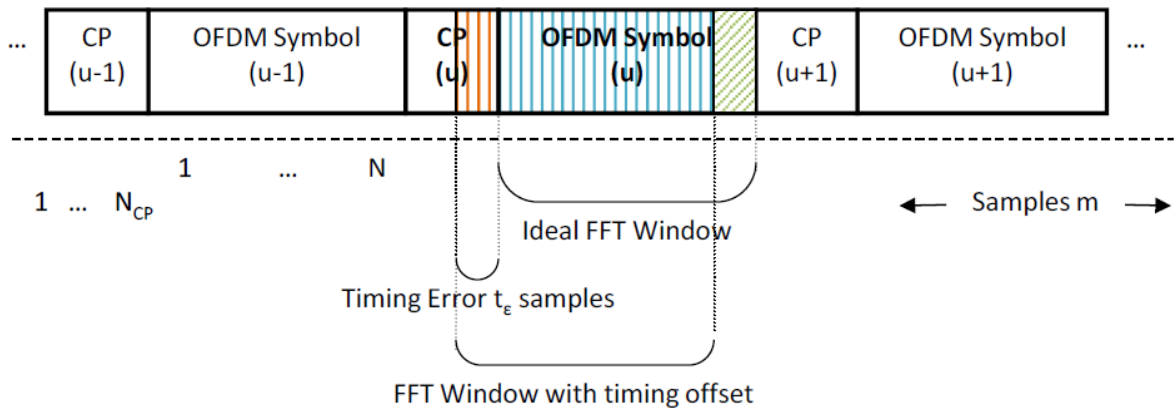


Figure 3-2 : Timing offset towards the CP (to the left) [11]

The demodulated OFDM signal affected by time offset in the direction of symbol's own cyclic prefix is given in Eq. (2), for case when $t_\varepsilon < N_{CP}$.

$$\hat{a}_{u',k'} = a_{u',k'} e^{-j2\pi \frac{k't_e}{N}} \quad (3.3)$$

Because of the cyclic prefix' presence, the orthogonality is preserved and ISI and ICI terms have disappeared. The timing error towards the cyclic prefix results therefore in pure phase shift.

3.1.2 Time Offset in WPM

The WPM transceivers do not apply guard intervals and therefore the direction of time offset is inconsequential. The demodulated signal under influence of time offset t_e can be written as:

$$\begin{aligned} \hat{a}_{u',k'} &= \sum_n R(n) \xi_{\log_2(N)}^{k'} (u'N - n + t_e) \\ &= \sum_n \sum_u \sum_{k=0}^{N-1} a_{u,k} \xi_{\log_2(N)}^k (n - uN) \xi_{\log_2(N)}^{k'} (u'N - n + t_e) \\ &= \sum_u \sum_{k=0}^{N-1} a_{u,k} \left(\sum_n \xi_{\log_2(N)}^k (n - uN) \xi_{\log_2(N)}^{k'} (u'N - n + t_e) \right) \end{aligned} \quad (3.4)$$

In order to shorten the derivation the following notation is defined:

$$\Omega_{k,k'}^{u,u'}(t_e) = \sum_n \xi_{\log_2(N)}^k (n - uN) \xi_{\log_2(N)}^{k'} (u'N - n + t_e) \quad (3.5)$$

Equation (3.5) represents the autocorrelation and the cross-correlation of the WPM waveforms. When $k = k'$ the two subcarrier waveforms are time-reversed images of each other and (3.5) gives the autocorrelation sequence of the waveform k . In the other cases when $k \neq k'$ the two waveforms correspond to different subcarriers and (3.5) stands for crosscorrelation between waveforms k and k' .

Using Eq. (3.4) and (3.5) we can now express the output of the WPM receiver for the k -th subcarrier and u -th WPM symbol as:

$$\hat{a}_{u',k'} = \underbrace{a_{u',k'} \Omega_{k',k'}^{u',u'}}_{\text{Useful Signal}} + \underbrace{\sum_{u;u \neq u'} a_{u,k'} \Omega_{k',k'}^{u,u'}}_{\text{ISI}} + \underbrace{\sum_u \sum_{k=0; k \neq k'}^{N-1} a_{u,k} \Omega_{k,k'}^{u,u'}}_{\text{ICI}} \quad (3.6)$$

In Eq. (3.6) the first term stands for attenuated useful signal. The second term gives the ISI due to symbols transmitted on the same subchannel and the third term denotes ICI measured over the whole frame.

The received constellation points of WPM under time synchronization errors do not experience linear phase rotation, opposed to OFDM where rotation of constellation points is proportional to subcarrier index. The WPM signal in presence of timing error will however be attenuated and it will suffer from ISI and ICI.

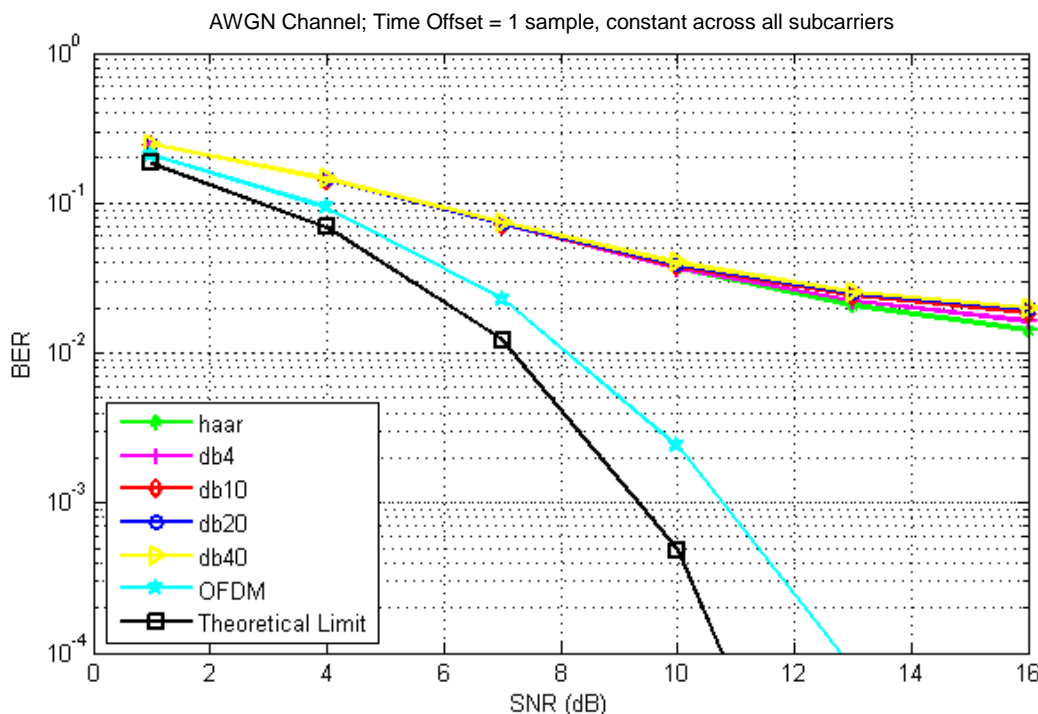
3.1.3 Numerical Results for Time Offset

The performances of WPM in presence of timing synchronization errors are investigated by means of simulations. The time offset is modeled as a discrete uniform distribution with integer value, i.e. 1 sample. Also in this simulation we include OFDM and theoretical AWGN BER as reference. We use cyclic prefix of 16 samples that is placed in front of OFDM symbols, while in WPM we don't use any guard interval.

Due to utilization of cyclic prefix the spectral efficiency of OFDM is decreased by 12.5% while spectral efficiency of WPM has remained unchanged. Finally, we employ the oversampling in order to magnify the difference in performance between various systems and wavelets. An overview of simulation parameters is given in table 3-1 through 3-4, while the respective results are shown in figure 3.3 through 3.6.

Table 3-1 : WPM Time Offset Simulation with Various Filter Length

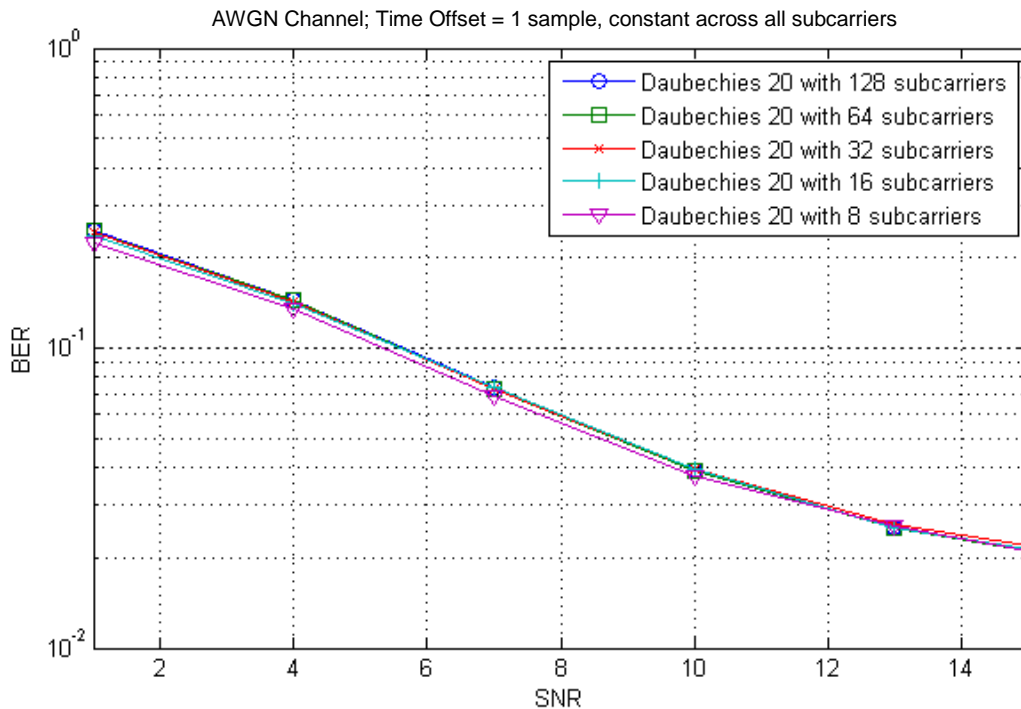
Simulation Parameters	
Wavelet Type	Daubechies
Wavelet Filter Length	2 (Haar), 4, 10, 20, 40
Number of Subcarriers	128
Number of Multicarrier Symbols per Frame	30
Modulation	QPSK
Channel	AWGN
Oversampling Factor	10
Time Offset (in sample)	$t_\varepsilon = 1$

**Figure 3-3 : WPM Time Offset Performance with Various Filter Length**

From figure 3-3 we can see that the OFDM system performs much better under time synchronization errors when compared to the WPM. This is due to cyclic prefix which increases robustness to channel spreading. The WPM cannot profit from these revisions and therefore show poor performance in presence of timing error. There is a slight degradation of BER performance when the wavelet filter is longer, mainly in the high SNR region.

Table 3-2 : WPM Time Offset Simulation with Various Number of Subcarriers

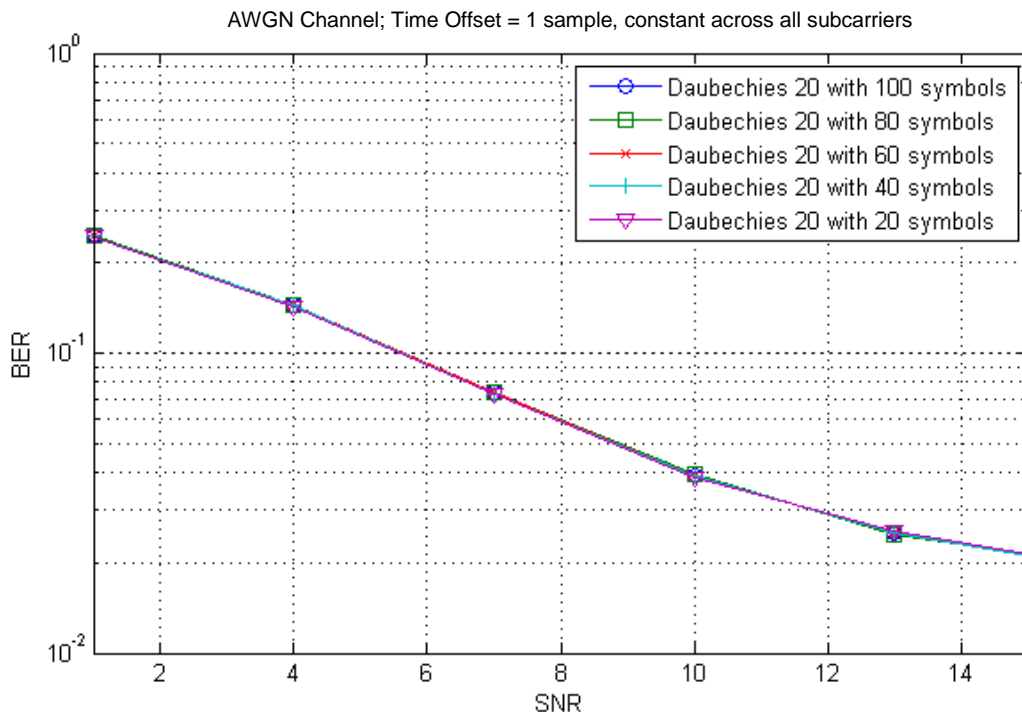
Simulation Parameters	
Wavelet Type	Daubechies
Wavelet Filter Length	20
Number of Subcarriers	128, 64, 32, 16, 8
Number of Multicarrier Symbols per Frame	30
Modulation	QPSK
Channel	AWGN
Oversampling Factor	10
Time Offset (in sample)	$t_\epsilon = 1$

**Figure 3-4 : WPM Time Offset Performance with Various Number of Subcarriers**

In figure 3-4, we compare a different number of subcarriers in WPM. Although the performance of each subject under study is slightly different, it can be seen that the scenario with larger number of subcarriers performs better. Although the effect is not significant, this is understandable because when more subcarriers are utilized, the symbol duration will also become longer and it will be beneficial in combating instantaneous fading and time offset.

Table 3-3 : WPM Time Offset Simulation with Various Number of Symbols

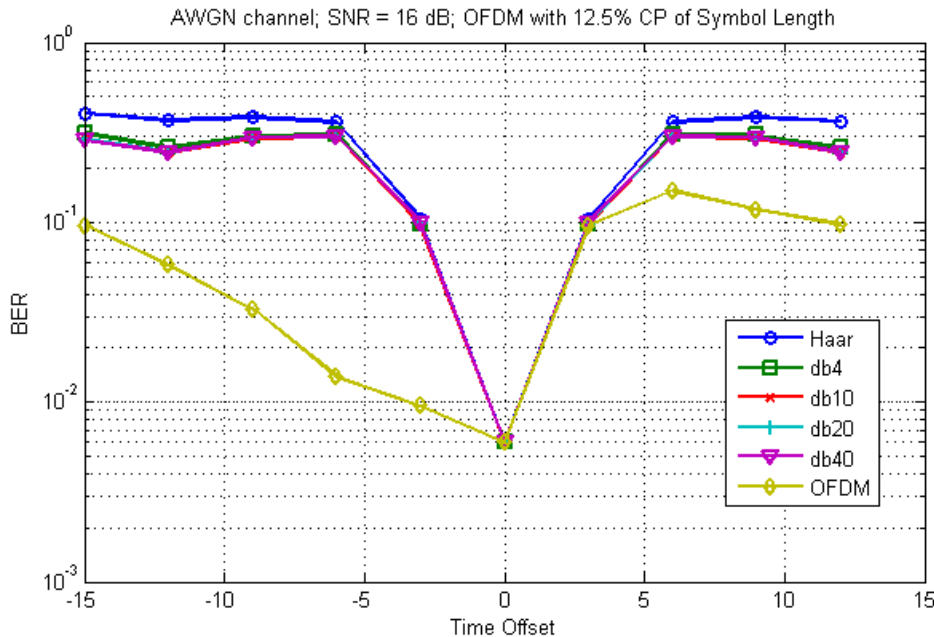
Simulation Parameters	
Wavelet Type	Daubechies
Wavelet Filter Length	20
Number of Subcarriers	128
Number of Multicarrier Symbols per Frame	100, 80, 60, 40, 20
Modulation	QPSK
Channel	AWGN
Oversampling Factor	10
Time Offset (in sample)	$t_\varepsilon = 1$

**Figure 3-5 : WPM Time Offset Performance with Various Number of Symbols**

In other hand, from figure 3-5 we can see the effects of various number of symbols to the performance, which is negligible. It can be concluded that there isn't any direct relation of the number of symbols to the performance.

Table 3-4 : WPM Time Offset Simulation with Various Time Offsets

Simulation Parameters	
Wavelet Type	Daubechies
Wavelet Filter Length	20
Number of Subcarriers	128
Number of Multicarrier Symbols per Frame	100
Modulation	QPSK
Channel	AWGN
Oversampling Factor	10
Time Offset (in sample)	$-1.5 \leq t_e \leq 1.5$

**Figure 3-6 : WPM Time Offset Performance with Various Time Offsets**

In figure 3-6, performance with various time offset can be observed. The SNR is kept fixed at 16 dB and we compare different length of wavelet filters. The result align well with the previous result from figure 3-3. The wavelet filters with longer length suffer from slight performance degradation in almost any given time offset. The BER curves of WPM are almost perfect mirror images with respect to the origin. This does not hold for OFDM, since we can see clearly that the negative timing offset (towards the own cyclic prefix) result in much lower BER when compared to the positive timing offsets (away from the own cyclic prefix).

3.2 Frequency Offset in Multicarrier Modulation

The orthogonality between the subcarriers is maintained at the receiver only if the transmitter and receiver have the same reference frequency. Any offset in the frequency will result in loss of orthogonality and hence in generation of interference. The interference is the most severe consequence of frequency offset but not the only one. Besides the interference term, frequency offsets initiates attenuation and phase rotation of each subcarrier.

Generally frequency offset can be caused by misalignment between receiver and transmitter local oscillator frequencies or due to Doppler shift. The Doppler frequency shift f_d is proportional to the subcarrier frequency $f(n)$ and the relative speed between the transmitter and the receiver v_r . The Doppler shift is expressed as:

$$f_d(n) = \frac{v_r f(n)}{c} \quad (3.7)$$

In (3.7) c denotes the speed of light and it is approximately equal to 3×10^8 m/s. The frequency of each subcarrier can be calculated by taking the sum of main carrier frequency f_c and baseband subcarrier frequency f_{sc} , i.e.:

$$f(n) = f_c \pm f_{sc}(n) \quad (3.8)$$

Using equation (3.7) and (3.8) we can express the relative frequency offset due to Doppler shift as the ratio between the actual frequency offset and inter-carrier spacing as:

$$f_\varepsilon = \frac{f_d(n)}{f_c \pm f_{sc}(n)} = \frac{v_r}{c} \quad (3.9)$$

The frequency offset can be modeled at the receiver by multiplying received time-domain signal by a complex exponential whose frequency component is equal to frequency offset value. If we assume that transmitted signal is given by $S(n)$, the received signal $R(n)$ can now be written as:

$$R(n) = S(n)e^{j2\pi f_\varepsilon n/N + \phi_0} + w(n) \quad (3.10)$$

In (3.10) f_ε denotes the relative frequency offset due to local oscillator mismatch or due to Doppler shift or due to combination of both. N stand for the total number of subcarriers, ϕ_0 is initial phase and w denotes additive white Gaussian noise (AWGN). Without loss of generality, we assume for the moment that $w(n) = 0$ and $\phi_0 = 0$.

3.2.1 Frequency Offset in OFDM

In OFDM the frequency offset prevents the perfect alignment of FFT bins with the peaks of the sinc pulses i.e. subcarriers. The FFT output corresponding to the k -th subcarrier can be written in this case as:

$$\begin{aligned} a_{k'} &= \frac{1}{N} \sum_{n=0}^{N-1} R(n) e^{-j2\pi \frac{k'n}{N}} \\ &= \frac{1}{N} \sum_{k=0}^{N-1} a_k \sum_{n=0}^{N-1} e^{j2\pi \frac{kn}{N}} e^{j2\pi f_e \frac{n}{N}} e^{-j2\pi \frac{k'n}{N}} \\ &= \frac{1}{N} \sum_{k=0}^{N-1} a_k \sum_{n=0}^{N-1} e^{j2\pi \frac{(k-k'+f_e)n}{N}} \end{aligned} \quad (3.11)$$

Using the geometric series properties the equation (3.11) can also be expressed as:

$$a_{k'} = \frac{1}{N} \sum_{k=0}^{N-1} a_k \frac{\sin(\pi(k-k'+f_e))}{\sin\left(\frac{\pi(k-k'+f_e)}{N}\right)} e^{j\pi\left(\frac{N-1}{N}\right)(k-k'+f_e)} \quad (3.12)$$

We can split equation (3.12) into two distinct parts:

$$a_{k'} = a_{k'} \frac{\sin(\pi f_e)}{N \sin\left(\frac{\pi f_e}{N}\right)} e^{j\pi\left(\frac{N-1}{N}\right)f_e} + \frac{1}{N} \sum_{k=0; k \neq k'}^{N-1} a_k \frac{\sin(\pi(k-k'+f_e))}{\sin\left(\frac{\pi(k-k'+f_e)}{N}\right)} e^{j\pi\left(\frac{N-1}{N}\right)(k-k'+f_e)} \quad (3.13)$$

The first component of equation (3.13) stands for useful demodulated signal, which has been attenuated and phase shifted due to frequency offset. The second part of (3.13) contains the ICI term, in which contribute all other subcarriers.

3.2.2 Frequency Offset in WPM

The presence of the frequency offset in WPM transceiver cause the frequency misalignment between the waveforms of the transmitter and the receiver. The detected data at the WPM receiver in case of the frequency offset can be written for the k -th subcarrier and u -th symbol as [11]:

$$\begin{aligned} a_{u',k'} &= \sum_n R(n) \xi_{2 \log(N)}^{k'} (u' N - n) \\ &= \sum_n \sum_u \sum_{k=0}^{N-1} a_{f,k} \xi_{2 \log(N)}^k (n - u N) e^{j2\pi f_e \frac{n}{N}} \xi_{2 \log(N)}^{k'} (u' N - n) \\ &= \sum_u \sum_{k=0}^{N-1} a_{f,k} \left(\sum_n \xi_{2 \log(N)}^k (n - u N) e^{j2\pi f_e \frac{n}{N}} \xi_{2 \log(N)}^{k'} (u' N - n) \right) \end{aligned} \quad (3.14)$$

In order to shorten the derivation we are going to use different notation, first we can define:

$$\Omega_{k,k'}^{u,u'} = \sum_n \xi_{2\log(N)}^k (n - uN) e^{j2\pi f_c \frac{n}{N}} \xi_{2\log(N)}^{k'} (u'N - n) \quad (3.15)$$

Using equation (3.14) and (3.15) we can now express the output of the WPM receiver for the k -th subcarrier and u -th WPM symbol as [11]:

$$a_{u',k'} = a_{u',k} \Omega_{k,k'}^{u,u'} + \sum_{u;u \neq u'} a_{u,k} \Omega_{k,k'}^{u,u'} + \sum_u \sum_{k=0;k'}^{N-1} a_{u,k} \Omega_{k,k'}^{u,u'} \quad (3.16)$$

In equation (3.16) the first term stands for attenuated and rotated useful signal. The second term gives the ISI due to symbols transmitted on the same subchannel and the third term denotes ICI measured over the whole frame.

3.2.3 Numerical results for Frequency Offset

The performance of WPM with frequency offset has been investigated by means of computer simulations and compared to the well-known OFDM. The WPM transceiver is simulated with various transmission properties as shown in Table 3-5. To simplify the analysis, the channel is taken to be additive white Gaussian noise (AWGN) and no other distortions except frequency offset is introduced. QPSK is the modulation of choice and frame size is set to 100 multicarrier symbols, each consisting of 128 subcarriers. Furthermore, the simulated system has no error estimation or correction capabilities nor are guard intervals or guard bands used. An overview of simulation set-up is given in table 3-5 through 3-8, while the respective results are shown in figure 3.7 through 3.10.

Table 3-5 : WPM Frequency Offset Simulation with Various Filter Length

Simulation Parameters	
Wavelet Type	Daubechies
Wavelet Filter Length	2 (Haar), 4, 10, 20, 40
Number of Subcarriers	128
Number of Multicarrier Symbols per Frame	30
Modulation	QPSK
Channel	AWGN
Oversampling Factor	10
Frequency Offset	$\Delta f = 0.1$

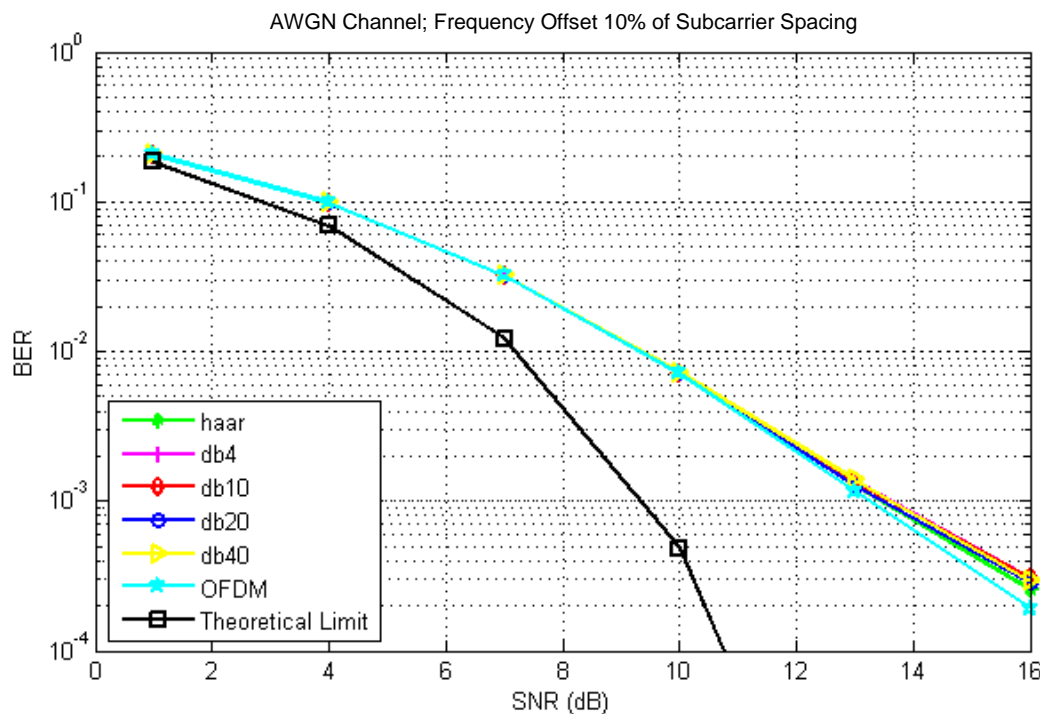
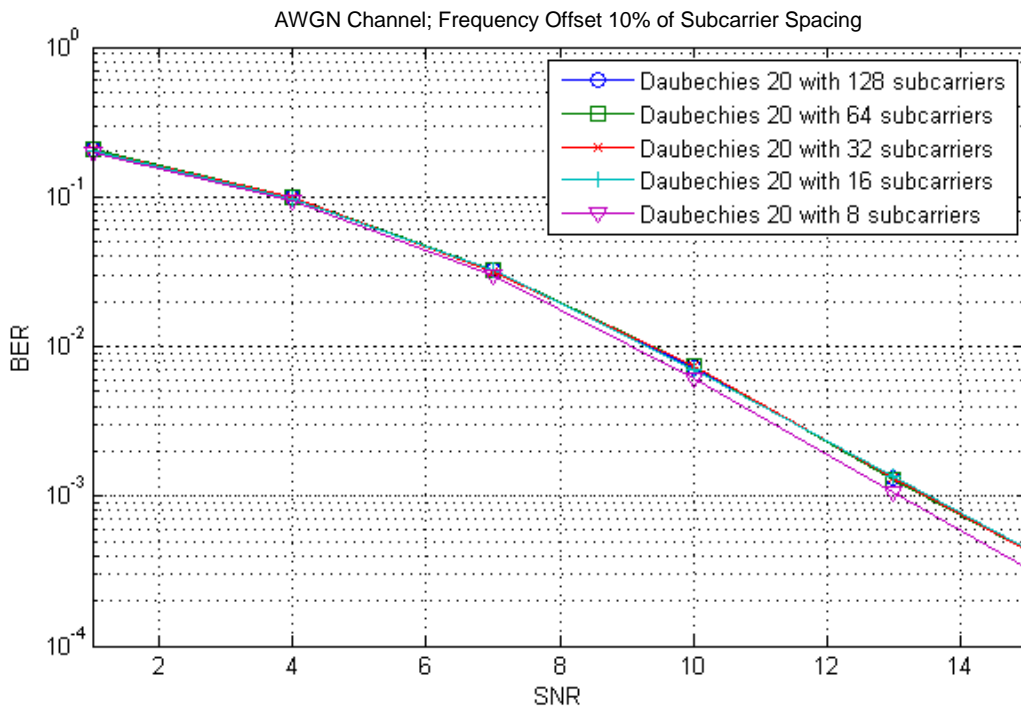
**Figure 3-7 : WPM Frequency Offset Performance with Various Filter Length**

Figure 3.7 illustrates the bit error rate (BER) of OFDM and WPM transceivers with relative frequency offset of 10% with regard to subcarrier spacing. BER curves of different wavelets and OFDM show similar performance but due to frequency offset they all lie far from theoretical curve.

Table 3-6 : WPM Frequency Offset Simulation with Various Number of Subcarriers

Simulation Parameters	
Wavelet Type	Daubechies
Wavelet Filter Length	20
Number of Subcarriers	128, 64, 32, 16, 8
Number of Multicarrier Symbols per Frame	30
Modulation	QPSK
Channel	AWGN
Oversampling Factor	10
Frequency Offset	$\Delta f = 0.1$

**Figure 3-8 : WPM Frequency Offset Performance with Various Number of Subcarriers**

The figure 3.8 is obtained during simulation where we investigate the influence of the amount of subcarriers in combination with frequency offset on the BER. All WPM transceivers are now simulated with the same wavelet but with different number of subcarriers. We arbitrarily chose the Daubechies wavelet with 20 coefficients. Furthermore the relative frequency offset is set to 10% and again we use AWGN channel.

The degradation of WPM 's BER in the presence of frequency offset is dependent on the number of subcarriers. This is straightforward when the absolute frequency offset is fixed [11], as for the more subcarriers in a given bandwidth the subcarrier spacing decreases and hence the relative frequency offset increases. However, in the figure 3.8 the relative frequency offset with respect to inter-carrier spacing is kept constant and there are still noticeable differences in the number of subcarriers used. The WPM with more subcarriers are slightly more susceptible to the frequency offset. This sensitivity decreases with increasing the number of subcarriers. From figure 3.8 we can also see that the performances of WPM with 64 and 128 subcarriers are almost identical for a given relative frequency offset.

Table 3-7 : WPM Frequency Offset Simulation with Various Number of Symbols

Simulation Parameters	
Wavelet Type	Daubechies
Wavelet Filter Length	20
Number of Subcarriers	128
Number of Multicarrier Symbols per Frame	100, 80, 60, 40, 20
Modulation	QPSK
Channel	AWGN
Oversampling Factor	10
Frequency Offset	$\Delta f = 0.1$

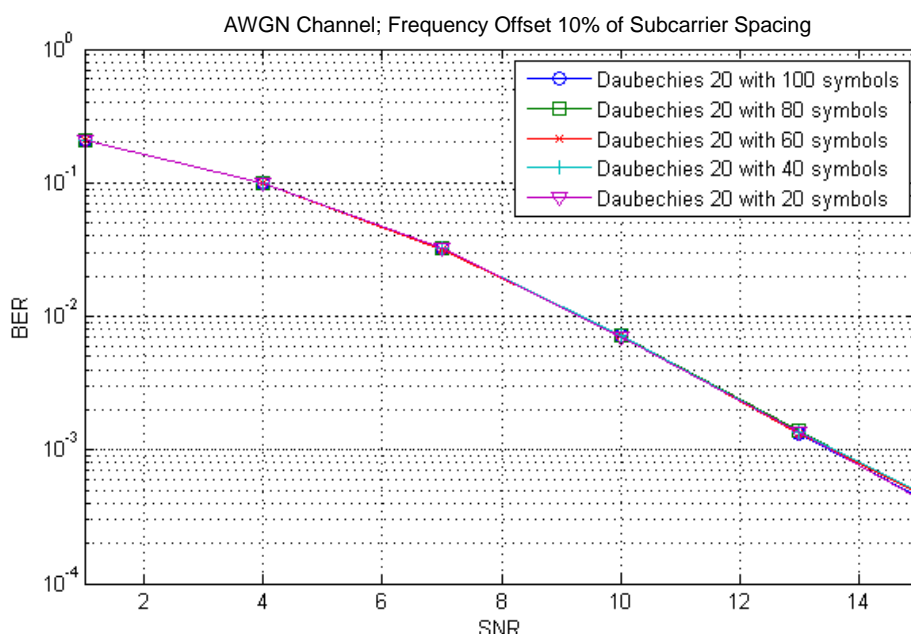
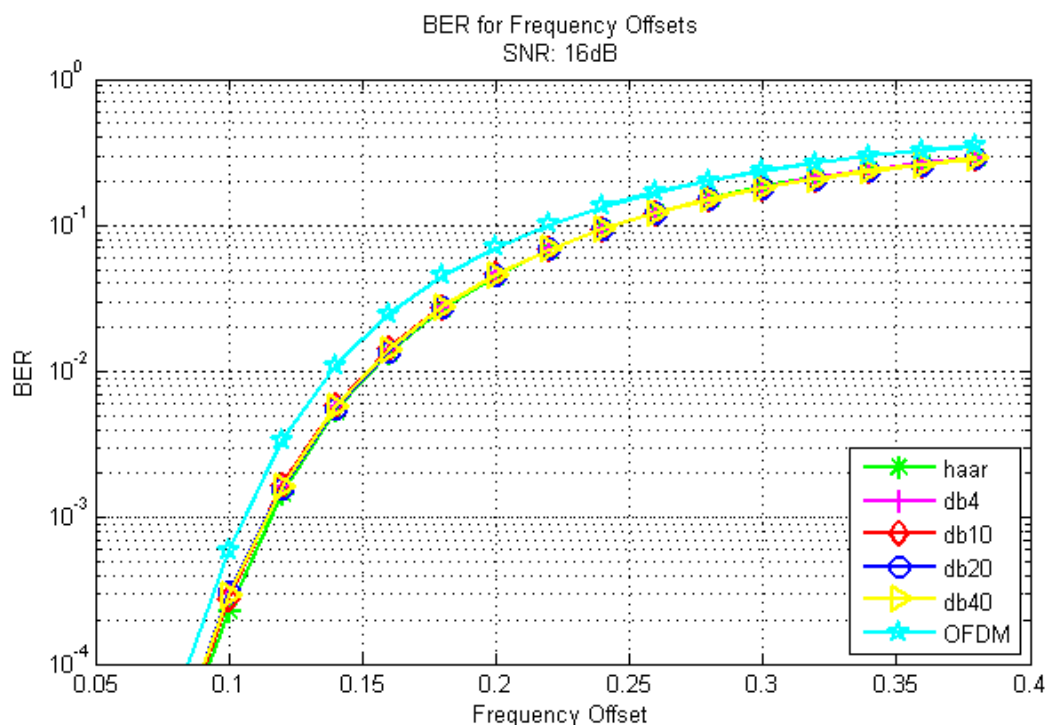


Figure 3-9 : WPM Frequency Offset Performance with Various Number of Symbols

Table 3-8 : WPM Frequency Offset Simulation with Various Frequency Offsets

Simulation Parameters	
Wavelet Type	Daubechies
Wavelet Filter Length	20
Number of Subcarriers	128
Number of Multicarrier Symbols per Frame	100, 80, 60, 40, 20
Modulation	QPSK
Channel	AWGN
Oversampling Factor	10
Frequency Offset	$0.05 \leq \Delta f \leq 0.4$

**Figure 3-10 : WPM Frequency Offset Performance with Various Frequency Offsets**

[Synchronization Impairments]

Frequency offset in WPM does not only lead to ICI inside one symbol but across the whole frame. Therefore, it is important to see the effect of the frame size in combination with the frequency offset. Figure 3.8 shows that the amount of multicarrier symbols in a frame does not affect the performance of WPM in the presence of frequency offset.

In figure 3.10 the BER is shown for different values of relative frequency offset varying from 10% to 40%, relative to the subcarrier spacing. During this simulation we kept SNR constant at 16 dB. Again we can see that the performances of majority of the wavelets are very similar to that of OFDM, while Haar wavelet slightly outperforms other wavelets and OFDM. The figure 3.10 implies that WPM and OFDM are both very sensitive to the frequency offset, since small variations of frequency offset degrade the system performance significantly.

3.3 Summary of Synchronization Impairments

In this chapter we studied the effects of synchronization errors, mainly the effects of time offset and frequency offset, on WPM and OFDM transceivers. The frequency offset and phase noise lead to the loss of orthogonality and subcarriers begin to interfere with each other. In OFDM interference is limited to ICI but in WPM the frequency offset and phase noise cause ICI as well as ISI. The effect of time synchronization error was also discussed. Akin to OFDM, we have found that timing error in WPM contains two components: ICI and ISI. There is however significant difference between both schemes in presence of timing error. Namely, the ISI in OFDM arises only between successive symbols while in WPM a number of symbols interfere one with another.

The effects of frequency offset and time synchronization errors were also examined by the simulations studies. We choose a well-known wavelet (Daubechies) and apply various properties to study the effects of each properties to the performance of the system. The sensitivity of WPM and OFDM are quite similar in presence of frequency offset. However, time synchronization error is found to be a major drawback of WPM transceiver. The simulations have shown that OFDM has much lower BER under timing errors when compared to WPM, mainly due to use of cyclic prefix in OFDM. Therefore, in the case of OFDM without CP, the performance will be more or less the same with WPM.

After observing the performance of WPM in the presence of time and frequency offset, we can conclude that WPM is not as reliable as OFDM if there are any time synchronization impairments, and hence a time synchronization scheme is vitally needed. Therefore, in the next chapter we will present the synchronization method for WPM to reduce the destructive effect of time offset and frequency offset.

4 SYNCHRONIZATION IN WPM

In the previous chapters we have seen that the WPM's subcarriers overlap in both time and frequency domain. Therefore, unlike in OFDM, the use of simple guard interval in WPM cannot prevent ICI and ISI from occurring when symbols are not correctly aligned at the receiver. This phenomenon is also closely related to possible methods of synchronization in WPM. Many synchronization techniques in OFDM rely on the use of guard interval and cyclic prefix. Therefore most OFDM synchronization techniques deal with the design of preamble and utilization of the cyclic prefix itself.

Although WPM provides other benefits such as freedom to choose the shape and properties of the waveforms, but in case of synchronization we need a synchronization techniques for WPM that is independent of the use of guard interval and cyclic prefix. In this chapter, recent works in the synchronization of WPM as well as possible synchronization method for WPM without using guard interval or cyclic prefix will be discussed.

4.1 Time Synchronization in WPM

4.1.1 Recent Works in Time Synchronization for WPM

The available literature on synchronisation algorithms for WPM modulated signals is sparse in comparison with the DFT-based schemes like OFDM. Fortunately, some of the work done for other multicarrier modulation schemes can be readily adapted to WPM. The early-late method proposed by Louveaux et al. to synchronise their filter bank based modulation scheme for DSL [21] provides for instance a good framework to derive a solution for WPM. While the method has shown to be capable of presenting a very low jitter, it has however the disadvantage of requiring the receiver to calculate both the early and late samples in addition to the on-time output samples. This directly leads to a two fold increase of complexity due to synchronisation only. To overcome this issue, Vandendorpe et al. proposed a more advanced method in [26] working at a sample rate.

Luise et al. have derived a non-data aided synchronisation scheme for multirate wavelet modulation [27]-[28]. Their method was then extended by Fu et al. to support signal timing initial acquisition [29] as part of the work on synchronisation for fractal modulation [30]-[31]. Sablatash and Lodge chose instead to insert a reference sequence in order to achieve synchronisation for a WPM signal generated by any arbitrary tree structure [32]. The proposed method is unfortunately not easily scalable and rather computationally intensive.

One of the most recent methods is the work of Jamin [36], which addresses the time synchronization more specific in the fractional or subsampling domain. The Mueller and Muller (M&M) algorithm [34], originally introduced for SC modulation, is derived from the maximum likelihood function. The simplest approximation of the algorithm makes use of only two consecutive estimates $\bar{x}[l-1]$, $\bar{x}[l]$ and their corresponding symbols after the decision $x[l-1]$, $x[l]$, in which:

$$\Delta\tau_{MM}[l] = \bar{x}[l-1]x[l] - \bar{x}[l]x[l-1] \quad (4.1)$$

where $\Delta\tau_{MM}$ is the estimate of the sampling phase error. Equation (4.1), using the decision symbols x , belongs to the family of decision directed algorithms [35]. In this case, known data sequences can be used instead of the decision symbols. This is of particular interest since not having decision errors leads to a better performance especially at low SNR. From a practical point of view, this is rather easy to set up with multicarrier schemes as it is common to have some pilot subcarriers modulated with known data symbols.

However, since the Mueller and Muller algorithm has been designed for SC modulation, its adaptation to the WPM scheme requires further attention. Louveau et al. have actually adapted it to the CMFB modulation [26]. It is however noticeable that their derivation, despite the fact that it is based on empirical analysis, is also valid for other multicarrier schemes, including WPM. Independent of the scheme actually considered, a number of differences with the SC case must be emphasised. In multicarrier systems, the modulated symbols are only available at the transform output. Therefore the subcarrier symbols are only available at every M sampling periods T . This leads to a loop delay that is much higher than with typical SC scheme, hence limiting the minimum convergence time of the close loop system it is a part of. In addition, the subcarriers being by definition centred on a different subband of the overall channel, the sampling frequency offset estimation must therefore be evaluated on several subcarriers to increase robustness against frequency selective fading. We must therefore choose how to combine the different estimates.

Figure 4-1 illustrates the implementation scheme of Mueller and Muller algorithm, with α_i and α_i denotes the received signal and the pilot signal, respectively.

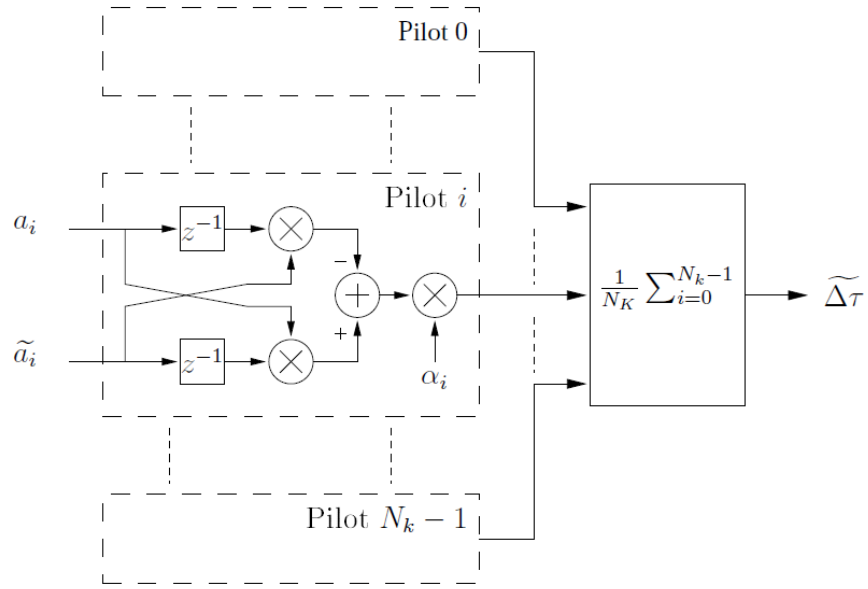


Figure 4-1 : Architecture of the M&M multicarrier timing offset estimator

Derivation in [26] has also shown that the sign of the sampling phase estimate is inverted for the subcarriers with an even index (subcarriers are indexed from 0 to $M-1$, with M being the transform size). Hence, the estimate on those subcarriers having an even index must be inverted before combination. Taking all these considerations into account, we can express the multicarrier sampling offset estimate $\Delta\tau$ as

$$\Delta\tau[l] = \sum_{k \in \mathbb{K}} \alpha_k (-1)^{k+1} \delta\tau_k[l] \quad (4.2)$$

where \mathbb{K} is the subset of the subcarrier indexes used to estimate the overall timing offset, α_k is a real positive weighing factor of subcarrier k .

The symbol $\delta\tau_k[l]$ denotes the timing error estimate on subcarrier k directly derived from Equation (4.2) which can be rewritten here as a function of the multicarrier symbols as

$$\delta\tau_k[l] = \alpha_{l-1,k} \cdot \alpha_{l,k} - \alpha_{l,k} \cdot \alpha_{l-1,k} \quad (4.3)$$

The introduction of the weighting factor α_k raises, of course, the question of how the estimates on the different subcarriers should be combined in order to obtain the final timing offset estimate. To clarify this particular point, Figure 4-2 plots the estimates $\delta\tau_k[l]$ of a WPM modulated signal as a function of the actual timing offset $\delta\tau$ for each subcarrier. This particular case makes use of a 16-point transform of the Daubechies order 6 wavelet.

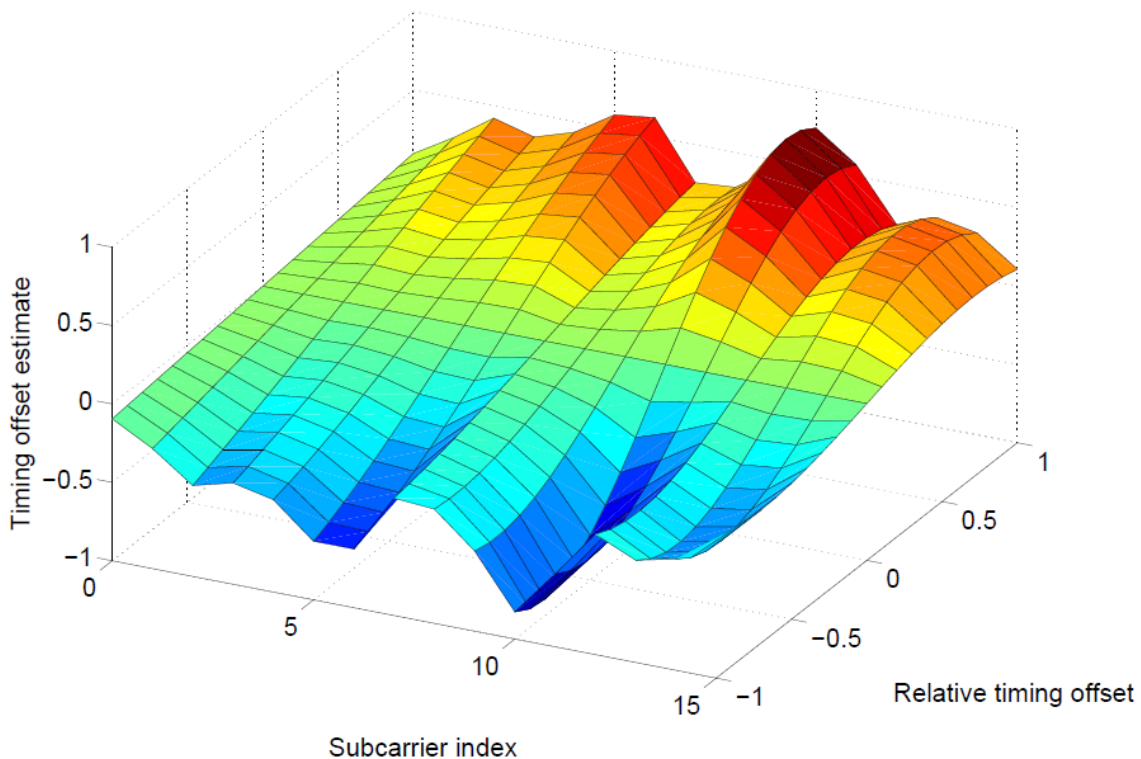


Figure 4-2 : Fractional time offset estimates of WPM (db6, 16 subcarriers)

It must be noted that, in this case, the subcarriers have been reordered in such a way that the higher the index k is, the higher the subcarrier centre frequency is. This is important as it clearly emphasises that the slope of the curve and its validity range are related to the position of the centre frequency of the subcarrier. In other words, the subcarriers of lower centre frequency can estimate the timing offset on a wider range, while the subcarriers with a higher centre frequency can estimate the timing offset more accurately. Altogether, this gives us an insight in order to decide how to choose the weighting factors α_k . Ultimately, the α_k could be calculated adaptively according to the value of the Timing Offset Estimator (TOE). At startup time, the range will be favoured. When the system has reached a low TOE and thus would be in tracking mode, the accuracy could be given a higher weight in the overall TOE instead. The approach chosen is intermediate as the α_k have been chosen in order for $\delta\tau_0$ to have a unity slope around the origin.

4.1.2 Proposed Method for Time Synchronization in WPM

While M&M method provides good performance in time synchronization, this method is more restricted to work in subsampling domain. To be implemented in a system, a more “coarse” synchronization method that is able to handle time offset larger than one sample is needed. This domain is where the proposed method will take place.

This proposed time synchronization method in Wavelet Packet Modulation (WPM) system uses correlation method in wavelet domain (after processed by the analysis filter bank). The method is based on Kjeldsen and Lindsey study about a feed-forward decision-directed approach to be implemented within a WPM demonstration prototype [33]. The method consists in regenerating the transmit signal at the receiver, with assumption that the received symbols are correctly detected. The algorithm then resamples the input signal in order to reach the best correlation between the locally generated signal and a delayed version of the received signal. This technique can be categorized as "decision directed synchronization" since it is based on using symbol decisions at the receiver to assist the synchronization process.

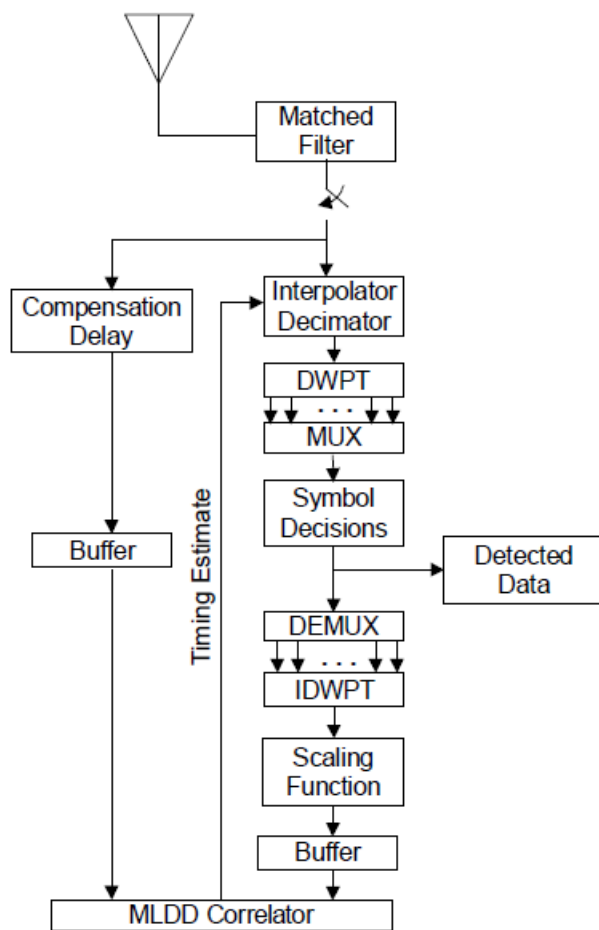


Figure 4-3 : WPM Symbol Synchronization Block Diagram

If the symbol decisions are correctly estimated, we can reconstitute the composite transmit WPM signal at the receiver based on these decisions. The reconstituted transmit signal is then correlated against a sliding window of signal samples out of a receiver matched filter. The correlation output

value will be the greatest when the window is optimally aligned between the directly received signal and the reconstituted transmit signal; an approximation to the "maximum likelihood criterion". The slide index (modulo reduced with respect to the transmit pulse period) corresponding to this maximum correlation value thereby informs the receiver which samples of the received signal correspond to the most interference-free symbol values.

$$\tau = \arg \max_{\tau} \sum_{i=1}^M \sum_{k=0}^{K-1} y_{i,k} g_i \hat{a}_{i,k} \quad (4.4)$$

where:

τ is the maximum likelihood timing estimator,

M is the number of subbands,

K is the observation window size in symbols,

$y_{i,k}$ is the k -th received complex symbol from the i -th analysis subband,

g_i is the known channel attenuation factor for the i -th analysis subband,

$\hat{a}_{i,k}$ is the k -th symbol decision out of the i -th analysis subband,

Although this form of the MLDD is mathematically simple, in the implementation timing estimator requires excessive computation at the branches of the receiver analysis filter bank, therefore it is not computationally efficient. We can make some adjustments to the computation to achieve more efficient implementation:

$$\tau = \arg \max_{\tau} \sum_{n=m}^{m+N} y_n \left[\sum_{i=1}^M \sum_{k=0}^{N_i} h_{i,k-n} g_i \hat{a}_{i,k} \right] \quad (4.5)$$

where:

y_n is the n -th sampled complex output from the receiver matched filter,

$h_{i,n}$ is the cascaded filter impulse response of the i -th analysis subband,

The rearrangement of terms in (4.5) allows the use of the sampled supersymbol values y_n (prior to decimation) instead of the M leaf values $y_{i,k}$. The inner summation group within the brackets can be easily formed by passing the product of the g_i channel attenuation factors and the slicer $\hat{a}_{i,k}$ symbol decisions through a synthesis bank equivalent to that of the transmitter. The result is then passed into a sliding correlator along with the delayed y_n supersymbol samples. Implementation of the MLDD timing estimator could "borrow" the synthesis filter bank (IDWPT) for use in synchronization during

packet reception and release this resource to the transmitter (in the same transceiver) to use when needed for the WPM transmission. This scheme is depicted in figure 4-3.

Based on simulation studies, a modification to (4.5) can decrease the variance and improve the convergence and stability properties of the WPM MLDD timing estimator. Instead of using the $\arg(\bullet)$ of the maximum likelihood function, the $\text{index}(\bullet)$ corresponding to modulo of operation of the maximum correlation slide and the N_s (which is number of samples per WPM pulse). The result is:

$$\tau = \text{index} \left[\max_{\tau} \sum_{n=m}^{m+N} y_n \sum_{i=1}^M \sum_{k=0}^{N_i} h_{i,k-n} g_i \hat{a}_{i,k} \right] \bmod N_s \quad (4.6)$$

where N_s is the number of samples per WPM pulse,

The MLDD timing estimator in (4.6) is suitable for WPM because it is based solely on correlation principles. Therefore, the difficulty in exploiting the non-conventional shape of the WPM symbols is not a concern. Instead of correlating all subcarriers, this method only correlate one specific subcarrier with its corresponding pilot. In real implementation, the pilot can be replaced by the decision symbol (after symbol constellation mapping) in the receiver, although this will result in degradation of performance in low SNR condition.

The algorithm works as follows. For a given observation window, the output of certain branch of the analysis filter bank is feeded to a sliding correlator window (which consists of the pilots of the corresponding subcarriers). This will give a series of result in the same size of the observation window. The largest value (the peak) of this result will correspond to specific value in the observation window, which is also the time offset estimates.

Assuming the input complex symbol constellations are independent and identically distributed (i.i.d.) and a sufficient symbol correlation window size is selected, the MLDD timing estimator should converge without requiring special training symbols [33]. A channel estimator is required to compute the channel attenuation factors, but for the sake of simplicity, in this scenario the channel are either not used or completely known to the receiver.

4.1.3 Numerical Results

The performance of proposed synchronisation algorithm is evaluated through simulation. The performance of the timing estimation is first illustrated by using simple scenario where the time offset is constant and known to receiver. For this particular simulation all the subcarriers are used as reference pilots for the purpose of illustration. The other parameters used are listed on table 4-1.

Table 4-1 : WPM Time Synchronization Simulation 1

Simulation Parameters	
Wavelet Type	Daubechies 20
Number of Subcarriers	128
Number of Multicarrier Symbols per Frame	30
Modulation	QPSK
Channel	AWGN
Oversampling Factor	1
Time Offset	$t_\epsilon = 2$

In this simulation, observation window size used, denoted by K in (4.4), is 25% of the symbol length. This is sufficient enough to give reliable estimation, as seen in the results. Although theoretically a larger observation window (e.g. 50% of symbol length) will give better performance, the difference is negligible, while the complexity of the process will increase drastically.

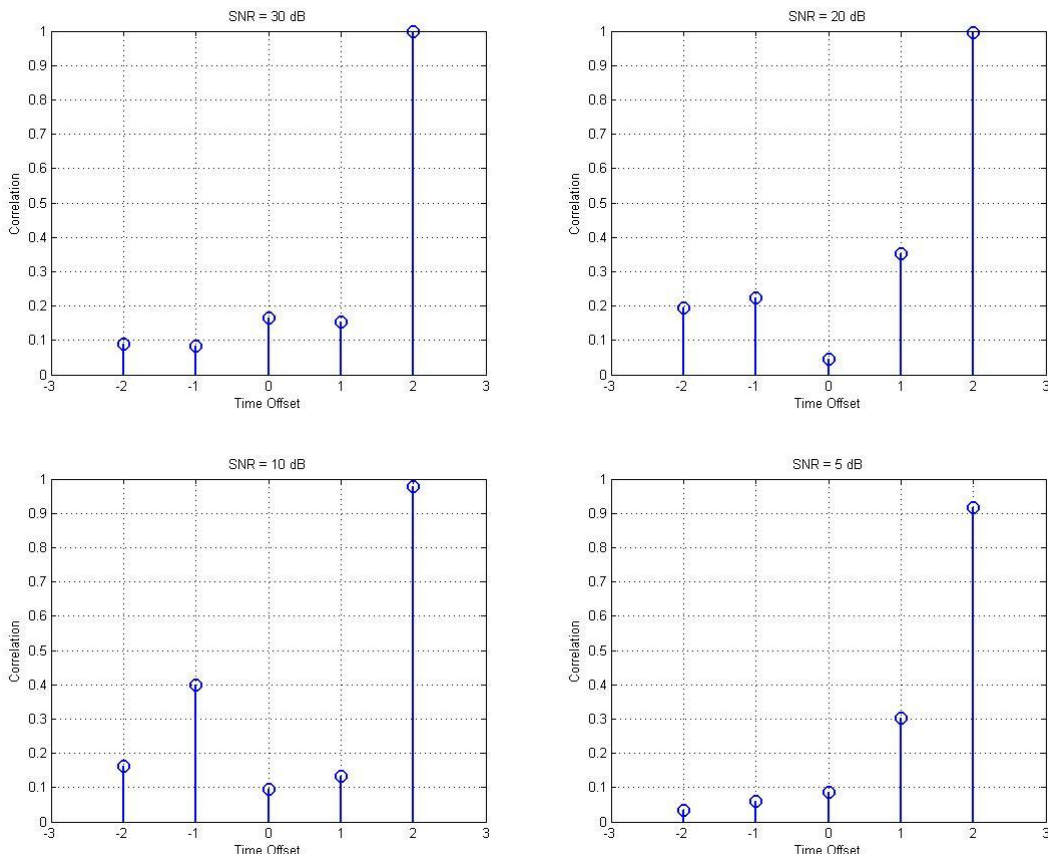


Figure 4-4 : Time Estimation with Time Offset = 2 and SNR: 30, 20, 10, and 5 dB

Time offset used in this simulation is 2 sample to the right and applied to all subcarriers in the frame. The correlation of the time estimates is shown for various SNR, the algorithm works successfully when the correlation peak is at the given time offset (2 sample).

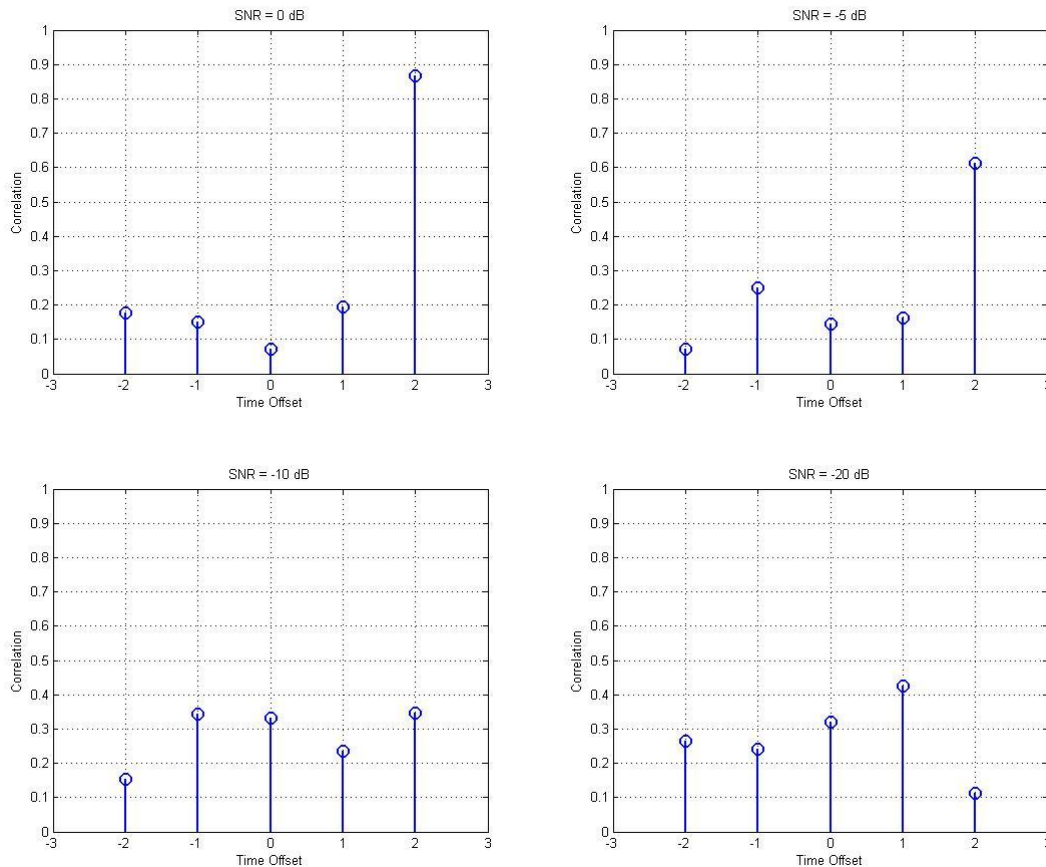


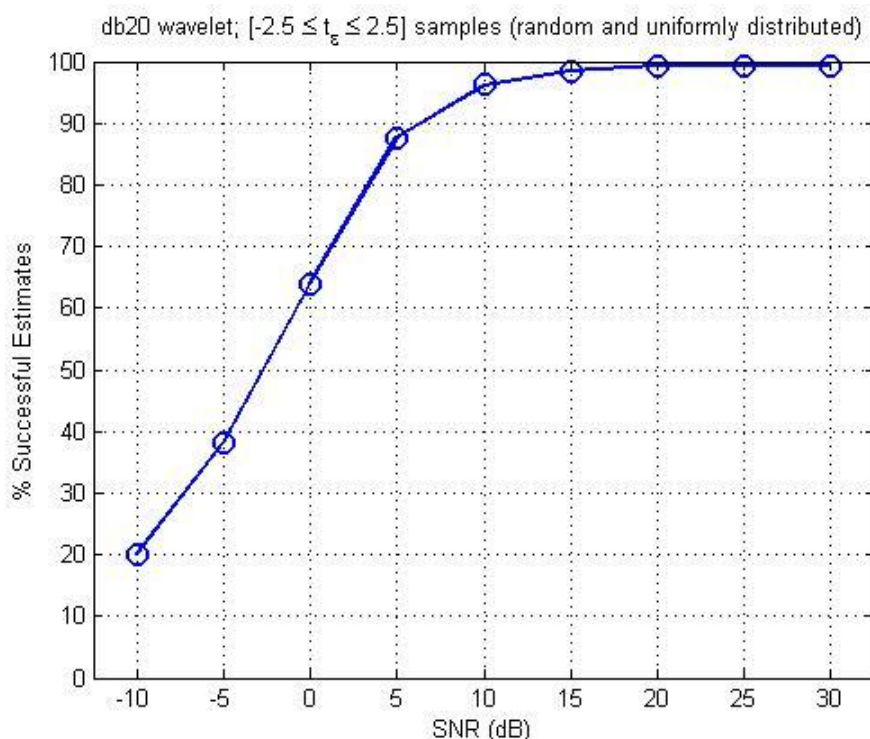
Figure 4-5 : Time Estimation with Time Offset = 2 and SNR: 0, -5, -10, and -20 dB

As seen in figure 4-4 and 4-5, the proposed method can still successfully estimate the given time offset in low region SNR (5 dB). But in lower SNR, such as SNR 0 and -5 dB, the performance degradation is significantly appeared. Although in this simulation the SNR 0 and -5 dB can be estimated successfully, this result might not accurately reflect the overall performance of the estimator since this simulation is done in singular basis (each result comes from one simulation). Therefore, a more complex simulation environment is needed.

Table 4-2 : WPM Time Synchronization Simulation 2

Simulation Parameters	
Wavelet Type	Daubechies 20
Number of Subcarriers	128
Number of Multicarrier Symbols per Frame	30
Modulation	QPSK
Channel	AWGN
Oversampling Factor	10
Time Offset	$-2.5 \leq t_e \leq 2.5$

The second simulation mainly uses same parameter as the first simulation, but in this scenario the time offset is generated randomly from -2.5 to 2.5 samples with uniform distribution and 0.1 sample interval. The receiver must estimate the correct time offset and the result will be averaged over 1000 independent iteration. The result is shown in Figure 4-6.

**Figure 4-6 : Percentage of Successful Estimation vs SNR**

The reason why fractional time offset is included in this simulation is to make the environment more realistic. In the implementation, the proposed method can be combined with M&M estimator to form a “Coarse-Fine” estimator. The proposed estimator acts as “coarse” estimator which synchronize the larger or integer part of the time offset, while M&M do the “fine tuning” to mitigate the fractional time offset.

Figure 4-6 reveals that the proposed estimator has more than 95% successful estimates (out of 1000 simulation) in SNR 10 dB or larger. To observe the effect of different length wavelet filters, simulations with Daubechies wavelets with filter length 2, 4, 10, and 20 are conducted. The results are depicted in Figure . It can be observed that the use of longer wavelet filter will result in a slight performance degradation, but in practical use this difference may become negligible.

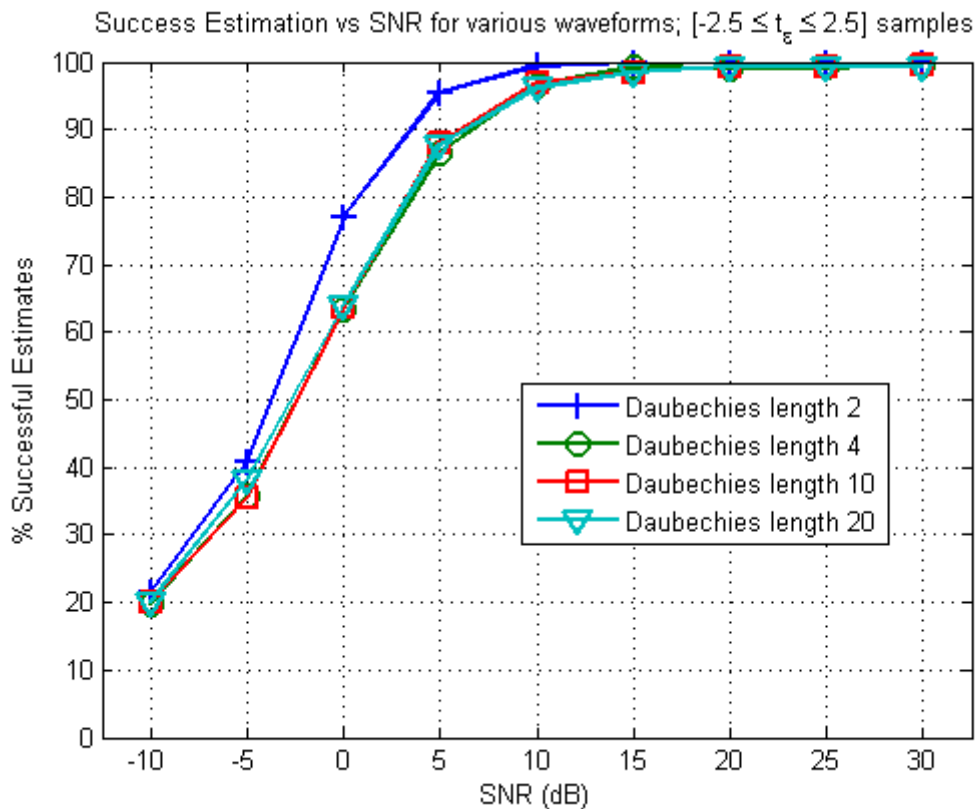


Figure 4-7 : Percentage of Successful Estimation for Different Wavelet Filter Length

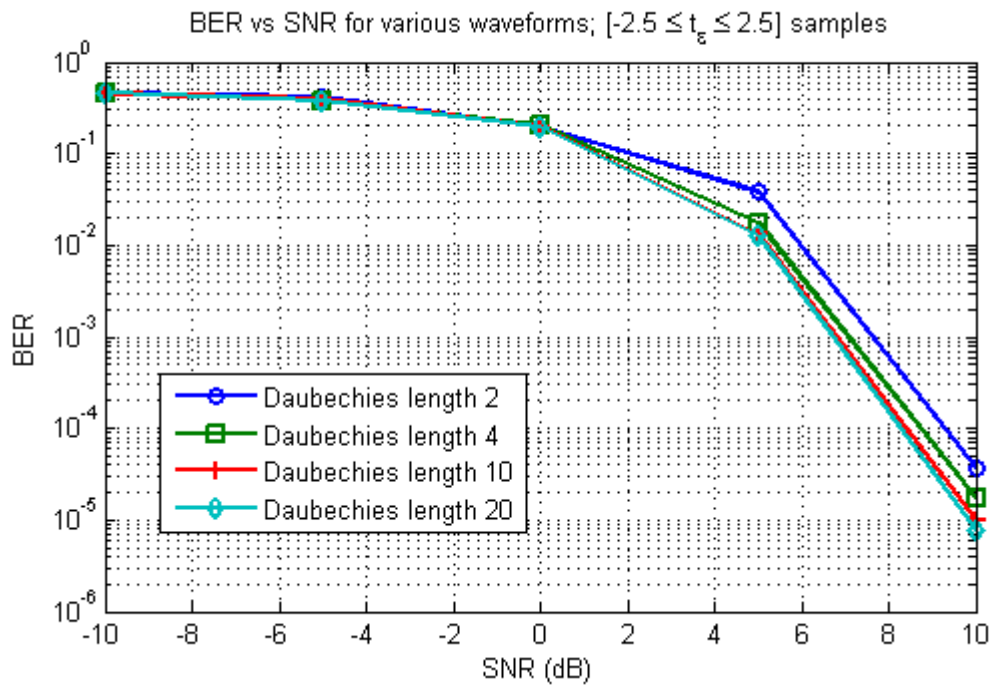


Figure 4-8 : Average BER for Different Wavelet Filter Length

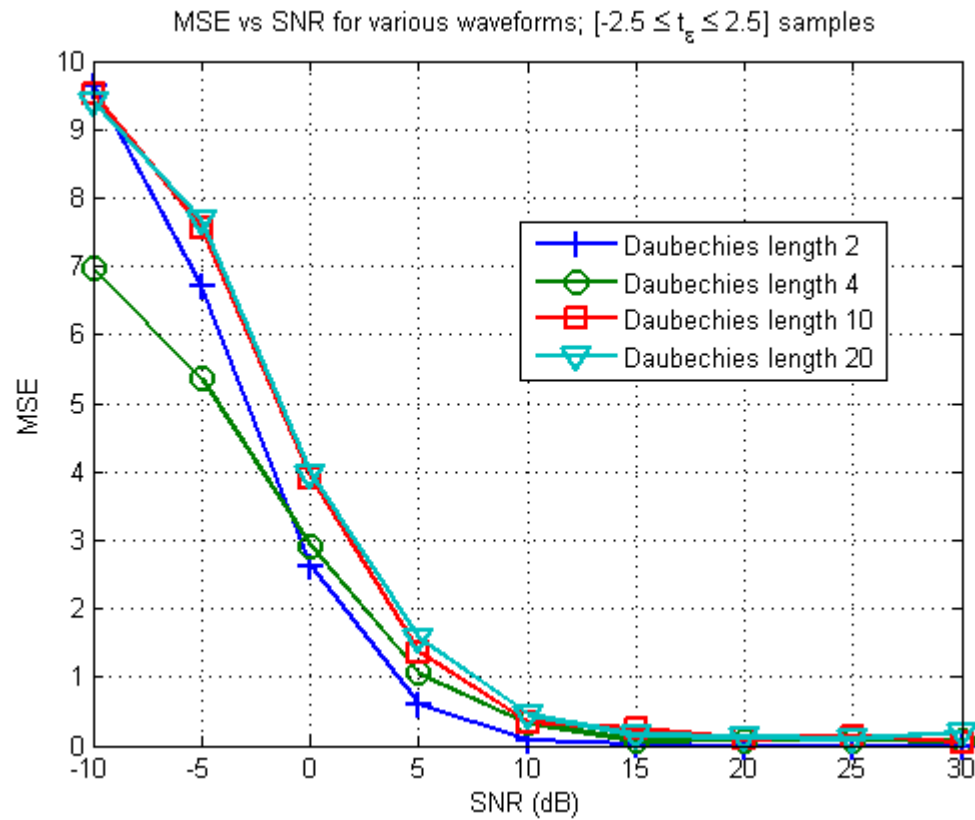


Figure 4-9 : Mean Square Error for Different Wavelet Filter Length

Figure 4-8 shows the performance of the WPM in presence of time synchronization error when the number of subcarriers and symbols in the frame is altered. For increasing length of wavelet filter the BER slightly decreases. In Figure 4-9, we can see the same trend continues where the performance of wavelet filter with longer length will degrade. i.e. has higher MSE value, especially in the 0 to 10 dB SNR region. In the high SNR region the difference then become once again negligible.

After estimation process is finished, the synchronization errors then can be corrected with digital interpolators (usually implemented as a bank of FIR filters known as a Farrow structure). It may be noted that in this experiment, the interpolator used are simply the inverse process of adding the offset to the signal transmitted. Therefore, although fractional offset can be estimated, the compensation implemented here is only work in integer domain. For a more accurate result, digital interpolator with Farrow structure will be needed, but this will be left for future works as the main objective of this simulation is to provide preliminary results in wavelet synchronization. According to Meyr et al., 4-tap FIR filters and a quadratic polynomial are sufficient for virtually all practical applications [37]. The notation x , μ , and y denote the input, step coefficient, and output, respectively while H_M , C_m , and Z denote the polyphase component, filter coefficient, and delay, respectively.

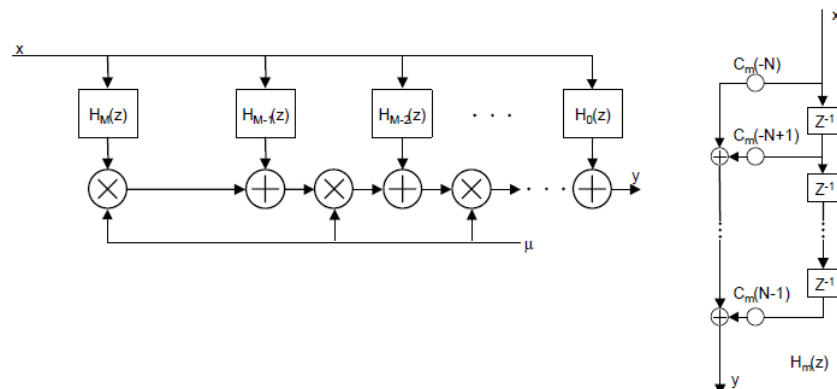


Figure 4-10 : Farrow Structure of the Polynomial Interpolator [37]

4.2 Frequency Synchronization in WPM

As discussed in the previous chapter, the orthogonality between the subcarriers is maintained at the receiver only if the transmitter and receiver have the same reference frequency. Any offset in the frequency will result in loss of orthogonality and hence in generation of interference. The interference is the most severe consequence of frequency offset but not the only one. Besides the interference term, frequency offsets initiates attenuation and phase rotation of each subcarrier. Generally frequency offset can be caused by misalignment between receiver and transmitter local oscillator frequencies or due to Doppler shift.

To mitigate the frequency offset, the first step is to do frequency offset estimation. One possible method to do this is by using M&M algorithm, that is also used in timing offset estimation. The motivation of using M&M algorithm in carrier frequency offset (CFO) estimation is because it is related to baud rate timing correction in single carrier systems, as proven in [28]. However, in this experiment, we only explore the estimation process, without meddling into the acquisition or interpolation process. Theoretically, by using a LMS algorithm for CFO estimate updating, the estimated CFO equals:

$$\hat{\Delta f}_{k+1} = \hat{\Delta f}_k - \mu_M \epsilon_{M,k} \quad (4.7)$$

Where μ_M is step size with M&M based acquisition. In the area of $-0.5 < \Delta f T < 0.5$ there will be an unique locking point, which make the LMS algorithm drive the CFO to zero [28].

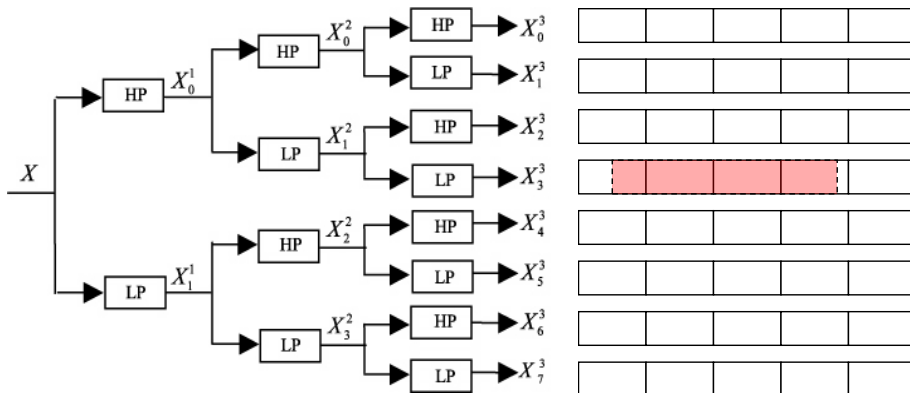


Figure 4-11 : M&M algorithm with correlation per subband basis (denoted in the shaded area)

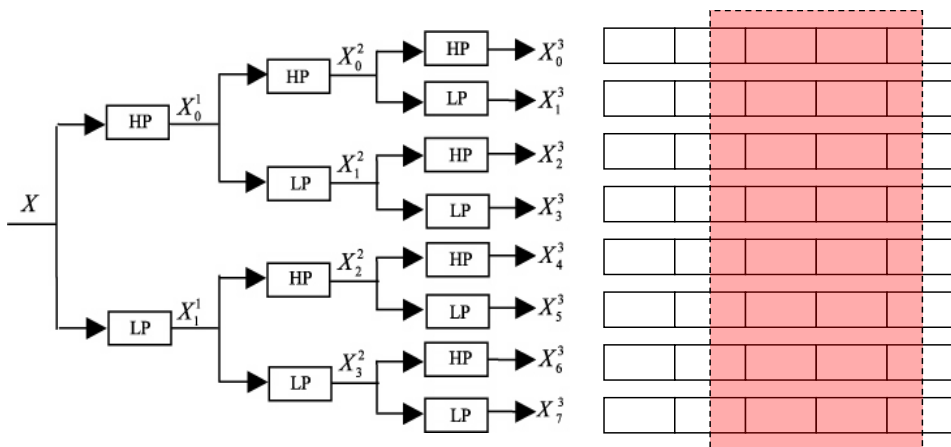


Figure 4-12 : M&M algorithm with correlation utilizes all subcarriers of the subbands (denoted in the shaded area)

Figure 4-11 and 4-12 show two different processes of calculating with the M&M algorithm. In estimating the time offset, we use the approach depicted by Figure 4-11, while in estimating frequency offset or CFO we use the approach illustrated by Figure 4-12. The simulation parameter used in this chapter summarized in Table .

Table 4-3 : WPM Frequency Synchronization Simulation

Simulation Parameters	
Wavelet Type	Daubechies 20
Number of Multicarrier Symbols per Frame	30
Modulation	QPSK
Channel	AWGN
Oversampling Factor	10
Frequency Offset	$-0.5 \leq \Delta f \leq 0.5$

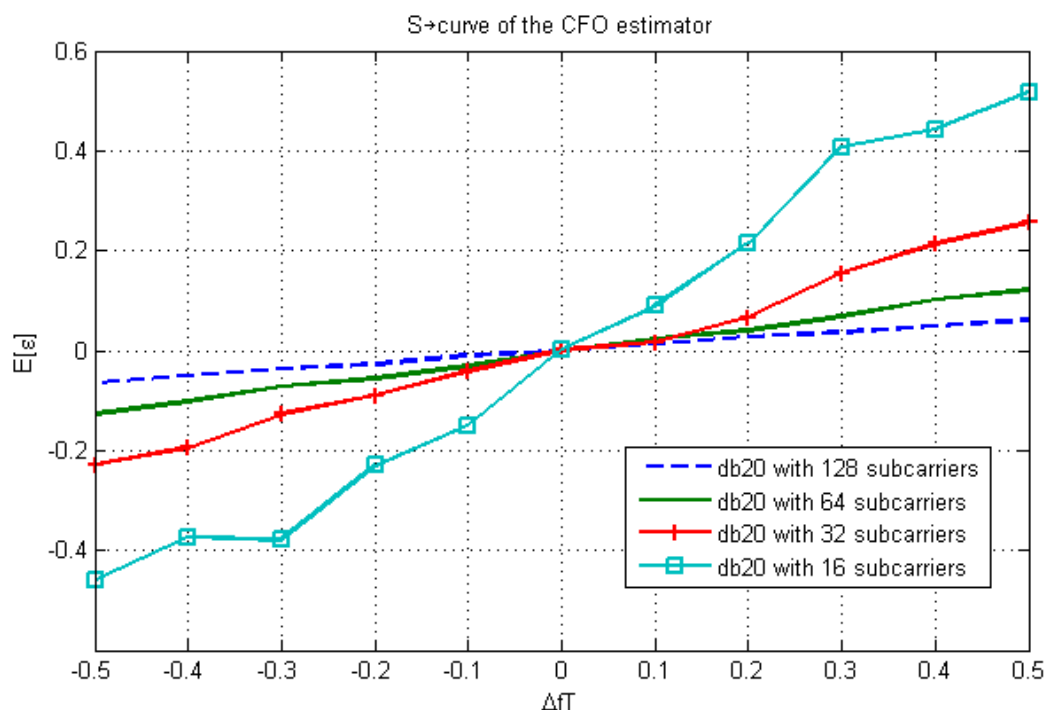


Figure 4-13 : S-curve of CFO estimator with perfect decisions and zero phase error

Figure 4-13 shows the error function for the estimated CFO as estimation error $E[\varepsilon]$ versus the normalized frequency offset ΔfT . It can be observed that the error performance is affected by the number of subcarriers in the modulation, and the better performance is shown by the less number of subcarrier being used. This aligns well with the fact that the more subcarrier utilized the less robust it will be against frequency imperfection, as discussed in Chapter 3.

4.3 Summary of WPM Synchronization

WPM lacks several of the waveform aspects that facilitate synchronization of OFDM. This is because the constituent elements of a WPM orthogonally-multiplexed symbol vary in shape across the sub-band scales. The scaling function that generates the wavelet basis family effectively “dilates” the pulse shape to create the orthogonality in time. There is no place for a guard interval or CP in WPM, so it is not possible to incorporate synchronization-aiding information on a similar periodic basis as in OFDM.

In this chapter we have presented synchronization techniques for WPM to overcome large or coarse timing errors based on Kjeldsen and Lindsey study of a feed-forward decision-directed approach. The method consists in re-generating the transmit signal at the receiver assuming the detected symbols are correct. The algorithm resamples the input signal in order to reach the best correlation between the locally generated signal and a delayed version of the received signal. The method's main advantages are its low implementation complexity and its flexibility. It can be made either data-aided or decision-directed, depending on the requirements of the application at hand. It proved to be robust as it is capable of tracking the time offset even in the presence of a large offset (more than 2 samples).

Another synchronization problem in WPM is the presence of frequency offset. Frequency offset can be caused by misalignment between receiver and transmitter local oscillator frequencies or due to Doppler shift. In OFDM and WPM the frequency offset prevents the perfect alignment of FFT bins with the peaks of the sinc pulses i.e. subcarriers. Mueller and Müller algorithm can also be used in estimating the frequency offset, as well as the time offset.

Further work on synchronization methods for WPM is necessary in order to enable and fully exploit its capability. The case of time varying multipath channel does for instance require further work. Alternatively, the methods proposed here can be combined with designing an orthogonal wavelet filter pair specifically optimised to show robustness to synchronization errors.

5 CONCLUSION

In this thesis work we have addressed the sensitivity of novel Wavelet Packed based Multi-Carrier (WPM) transmission system to the carrier frequency offset and time synchronization errors. Furthermore, we have proposed a synchronization method to estimate time and frequency offset, as the first step to mitigate those problems in WPM.

5.1 Key Research Conclusions

The core conclusions of this effort can be summarized in the following points:

- Spectral efficient multicarrier transceivers as WPM and OFDM are vulnerable to time offset which causes subcarriers to lose their mutual orthogonality and begin to interfere one with another. Under time synchronization errors OFDM can take advantage of cyclic prefix to greatly reduce the generation of interference as opposed to WPM which cannot benefit from such constructions due to time overlap of the symbols. Nevertheless, cyclic prefix in OFDM fails to prevent interference from occurring if offset value is larger than the size of the prefix or when offset is in the opposite direction with regard to symbol's own prefix. When parts of the neighboring symbols get erroneously selected at the OFDM or WPM receiver windows, the demodulated signal will be distorted by Inter Symbol Interference (ISI) and Inter Carrier Interference (ICI). In OFDM, ISI arises only due to neighboring multicarrier symbols, while in WPM more than two multicarrier symbols contribute to the ISI generation.
- In OFDM performance degradation due to frequency offset is limited to the interference among the subcarriers within one OFDM symbol (ICI), while in WPM subcarriers from multiple symbols interfere with each other (causing ICI + ISI). This dissimilarity in the interference behavior is due to the manner in which the subcarriers in wavelet and Fourier based systems are created. The signals generated by OFDM overlap only in frequency domain while WPM generated signals overlap in both frequency and time domain.
- Simulations studies have shown that the performance degradation of WPM and OFDM are quite similar in the presence of frequency offset. However, time synchronization error is found to be a

major drawback of WPM transceivers. Therefore, we focused our attention on the time synchronization error and attempted to find a solution for the large performance gap between WPM and OFDM transceivers under timing errors.

- As the first step to mitigate synchronization problem in WPM, we studied the possible methods of synchronization to be implemented in WPM system. Most of the methods we tried is derived from synchronization method in OFDM which doesn't utilize the cyclic prefix in the process. Among the methods, two have been emerged as the most suitable candidate for the WPM synchronization, namely the Mueller & Muller based algorithm and the Maximum Likelihood Decision Directed (MLDD) algorithm. We have tried both algorithms but the reported Jamin's results for Mueller & Muller based algorithm [36] were not reproducible. Thus we decided to move on with the MLDD approach which only relies on the correlation properties of the wavelet signals.
- While the synchronization method based on Mueller & Muller algorithm provides a good performance in time synchronization, this method is more restricted to work in subsampling domain. To be implemented in a system, a more "coarse" synchronization method that is able to handle time offset larger than one sample is needed. This domain is where the proposed method will take place. The proposed time synchronization method in Wavelet Packet Modulation (WPM) system uses correlation method in wavelet domain (after processed by the analysis filter bank). The method is based on Kjeldsen and Lindsey study [33] about a feed-forward decision-directed approach.

In this thesis work we study the effects of synchronization impairments, mainly time offset and frequency offset, to the performance of WPM and OFDM systems. Our simulation results show that the sensitivity of WPM and OFDM are quite similar in presence of frequency offset. However, time synchronization error is found to be a major drawback of WPM transceiver. This thesis work can be considered as a preliminary work to the complete design of synchronization algorithm specifically tailored for the WPM, as the method proposed in this thesis work is only derived from OFDM synchronization methods with some adjustments. Considering the great potential of WPM, time synchronization of WPM remains a challenging issue to solve in the future.

5.2 Recommendations for Further Research

Although the theory of wavelet transform has been well-evolved and documented over the past years, the use of wavelets in the telecommunication systems is still in the early stage of the development. Therefore, there remain several important issues and concepts that are worth investigating.

- The first suggestion concerns time offset correction. In this thesis the vulnerability of WPM to time synchronization errors was addressed and timing offset estimation method for WPM was

proposed and implemented. Nevertheless, the fact remains that we cannot use guard intervals because of the overlapping nature of WPM symbols, therefore only moderate timing errors are acceptable. For this reason, a robust frame synchronization algorithm is still needed to be developed, especially in the tracking process to correct large time offsets after estimated by the proposed method.

- Secondly is the complexity analysis of the synchronization methods. The complexity analysis of the proposed modified MLDD compared to the original MLDD can be necessary when it comes to implementation issues. It is also interesting to compare the complexity of the WPM synchronization algorithms with existing OFDM synchronization algorithms, which can be a useful reference in transceivers design.
- Next is regarding frequency offset correction in WPM, this thesis work only addresses the estimation of frequency offset. Therefore, a robust method of frequency tracking after the estimation is still need to be developed.
- The other synchronization problem not addressed in this thesis work is the phase noise that can be caused by thermal noise, causing the oscillator's central frequency to fluctuate a bit. The influence of the phase noise on multicarrier transmission can be divided into two parts: Common Phase Error and Interference. Phase noise can also cause the loss of orthogonality between subcarriers, therefore synchronization methods to mitigate phase noise are also needed in the successful implementation of WPM systems.
- Finally, in this thesis work, the synchronization impairments are tested one at a time to simplify the analysis, meaning that the time offset and frequency offset are assumed independent for each simulation. An interesting further research would be to implement a joint time-frequency synchronization methods and test them in a more realistic environment, such as wireless channels where the time and frequency offset can occur simultaneously, together with the fading and multipath, etc.

BIBLIOGRAPHY

- [1] S.Haykin, "Cognitive Radio: Brain-Empowered Wireless Communications", IEEE JSAC, Vol.23, No.2, pp.201-220, February 2005
- [2] J.Mitola, G.Q.Maguire, "Cognitive Radio: Making Software Radios More Personal", IEEE Personal Communications, Vol.6, No.4, pp.13-18, August 1999
- [3] A.Lindsey, "Wavelet Packet Modulation for Orthogonally Transmultiplexed Communications", IEEE Transaction on Communications, Vol.45, pp.1336-1339, May 1997
- [4] G.Wornell, "Emerging Applications of Multirate Signal Processing and Wavelets in Digital Communications", Proc. of IEEE, Vol.84, pp.586-603, April 1996
- [5] M.K.Lakshmanan, H.Nikookar, "A Review of Wavelets for Digital Wireless Communication", Springer Journal on Wireless Personal Communication, Vol.37, No.3-4, pp.387-420, May 2006
- [6] B.G.Negash, H.Nikookar, "Wavelet-based Multicarrier Transmission Over Multipath Wireless Channels", IEE Electronic Letters, Vol.36, No.21, pp.1787-1788, October 2000
- [7] M.K.Lakshmanan, H.Nikookar, "Wavelet Packet based Strategy to Mitigate Wideband Interference on Impulse Radio", IEEE (PIMRC 2007) Personal, Indoor and Mobile Radio Communications, pp.1-5, September 2007
- [8] S. Mallat, "A theory of multiresolution signal decomposition: the wavelet representation", IEEE Transactions on Pattern Analysis and Machine Intelligence, 11(7):674-693. 1989
- [9] Akansu et. al, "Wavelet and Subband Transforms: Fundamentals and Communication Applications", IEEE Communications Magazine, Vol. 35, pp. 104-115, Dec. 1997
- [10] C. S. Burrus, R. A. Gopinath, and H. Guo, "Introduction to Wavelets and Wavelet Transforms: A Primer", Prentice Hall, 1998
- [11] D.Karamehmedovic, "A Study of Synchronization Issues of Wavelet Packet based Multicarrier Modulation", M.Sc. Thesis, Delft University of Technology, 2009
- [12] Misiti et. al, "Wavelet Toolbox Documentation for MATLAB", Mathworks. 1997
- [13] C.R.N.Athaudage, "BER Sensitivity of OFDM Systems to Time Synchronization Error", in Proc. IEEE International Conference on Communication Systems (ICCS 2002), Vol.1, pp.42-46, November 2002

- [14] Y.Mostofi, D.C.Cox, "Mathematical Analysis of the Impact of Timing Synchronization Errors on the Performance of an OFDM System", IEEE Transaction on Communications, Vol.54, No.2, February 2002
- [15] D.Liu, Y.Tang, D.Sang, S.Li, "Impact of the Timing Error on BER Performance of TDD Pre-equalized OFDM System", in Proc. IEEE International Conference on Personal Wireless Communications (ICPWC _2000), Vol.1, pp.714-718, September 2004
- [16] D.Lee, K.Cheun, "Coarse Symbol Synchronization Algorithms for OFDM Systems in Multipath Channels", IEEE Communication Letters, Vol.6, No.10, pp.446-448, October 2002
- [17] M.Sandell, J.J.Beekm P.O.Brjesson, "Timing and Frequency Synchronization in OFDM Systems using the Cyclic Prefix", International Symposium on Synchronization, pp.16-19, 1995
- [18] M.Tanda, "Blind symbol-timing and frequency-offset estimation in OFDM systems with real data symbols", IEEE Transactions on Communications, Vol.52, No.10, pp.1609-1612, October 2004
- [19] A.J.Coulson, "Maximum likelihood synchronization for OFDM using a pilot symbol: algorithms", IEEE Journal on Selected Areas in Communications, Vol.19, No.12, pp. 2486-2494, December 2001
- [20] B. Yang, K.B.Letaief, R.S.Cheng , Z.Cao,"Timing recovery for OFDM transmission", IEEE Journal on Selected Areas in Communications, Vol.18, No.11, pp.2278-2291, November 2000
- [21] J. Louveaux, L. Vandendorpe, L. Cuvelier, and T. Pollet, "An earlylate timing recovery scheme for filter bank-based multicarrier transmission," IEEE Transactions on Communications, vol. 48, no. 10, pp. 1746-1754, October 2000
- [22] T.Pollet, M.van Bladel, M.Moeneclaey, "BER Sensitivity of OFDM Systems to Carrier Frequency Offset and Wiener Phase Noise", IEEE Transaction on Communications, Vol.43, pp.191-193, April 1995
- [23] H.Nikookar, R.Prasad, "On the Sensitivity of Multicarrier Transmission over Multipath Channels to Phase Noise and Frequency Offset", in Proc. 7th IEEE International Symposium Personal, Indoor Mobile Radio Communication (PIMRC '96), Vol.1, pp.68-72, October 1996
- [24] J.Armstrong, "Analysis of New and Existing Methods of Reducing Intercarrier Interference Due to Frequency Offset in OFDM", IEEE Transaction on Communications, Vol.47, No.3, pp.365-369, March 1999
- [25] P.H.Moose, "A Technique for Orthogonal Frequency Division Multiplexing Frequency Offset Correction", IEEE Transaction on Communications, Vol.42, No.10, pp.2908-2914, October 1994
- [26] J. Louveaux, L. Cuvelier, L. Vandendorpe, and T. Pollet, "Baud rate timing recovery scheme for filter bank-based multicarrier transmission," IEEE Transactions on Communications, vol. 51, no. 4, pp. 652-663, April 2003
- [27] M. Luise, M. Marselli, and R. Reggiannini, "Symbol timing recovery for wavelet-based linear modulations," in Global Communication Conference (GLOBECOM), 1999, pp. 2513-2517

- [28] M. Luise, M. Marselli, and R. Reggiannini, "Clock synchronisation for wavelet-based multirate transmissions," IEEE Transactions on Communications, vol. 48, no. 6, pp. 1047-1054, June 2000
- [29] C.-M. Fu, W.-L. Hwang, and C.-L. Huang, "Timing acquisition for wavelet-based multirate transmissions," in Proceedings of Global Communication Conference (GLOBECOM), vol. 4, December 2003, pp. 2208-2212
- [30] C.-M. Fu, W.-L. Hwang, and C.-L. Huang, "Clock synchronization for fractal modulation," in Proceedings of International Conference on Acoustics, Speech and Signal Processing, vol. 3, May 13-17 2002, pp. 2809-2812
- [31] C.-M. Fu, W.-L. Hwang, and C.-L. Huang, "Timing acquisition for fractal modulation in gaussian white and 1/f channels," in Proceedings of International Conference on Acoustics, Speech and Signal Processing, vol. 4, May 17-21 2004, pp. 841-844
- [32] M. Sablatash and J. Lodge, "Design of a synchronization scheme for a bandwidth-on-demand multiplexer-demultiplexer pair based on wavelet packet tree filter banks," in International Conference on Acoustics, Speech and Signal Processing, vol. 4, 1999, pp. 2211-2214
- [33] E. Kjeldsen and A. Lindsey, "Receiver timing recovery for adaptive wavelet packet modulated signals," in Conference Record of the 36th Asilomar Conference on Signals, Systems and Computers, vol. 1, April 2002, pp. 92-96
- [34] K. H. Mueller and M. Muller, "Timing recovery in digital synchronous data receivers," IEEE Transactions on Communications, vol. COM-24, no. 5, pp. 516-531, May 1976
- [35] J. G. Proakis, *Digital Communications*, 3rd ed. McGraw Hill International Editions, 1995
- [36] A. Jamin, P. Mähönen, "Mueller & Müller algorithm based synchronisation for wavelet packet modulation," IWCNC 2006: 1195-1200
- [37] H. Meyr, M. Moeneclaey, and S. A. Fechtel, *Digital communication Receivers*. Wiley Interscience, 1997
- [38] D.Karamehmedović, M.K.Lakshmanan, H.Nikookar, "Performance of Wavelet Packet Modulation (WPM) and OFDM in the Presence of Carrier Frequency Offset and Phase Noise", in Proc. European Wireless Technology Conference (EuWiT), October 2008
- [39] D.Karamehmedović, M.K.Lakshmanan, H.Nikookar, "Performance Degradation Study of Wavelet Packet based Multicarrier Modulation Under Time Synchronization Errors", in Proc. International Wireless Personal Multimedia Communications Symposium (WPMC), September 2008
- [40] D.Karamehmedović, M.K.Lakshmanan, H.Nikookar, "Phase Noise Effects on the Performance of Wavelet Packet Multi-Carrier Modulation", Wireless Communication Society, Vehicular Technology, Information Theory and Aerospace & Electric System Technology (Wireless VITAE), May 2009
- [41] D.Karamehmedović, M.K.Lakshmanan, H.Nikookar, "Optimal Wavelet Packet Design for Multicarrier Modulation with Time Synchronization Error", IEEE Global Communications Conference (Globecom 2009)

